DEFORMATION CHARACTERISTICS OF DUPLEX FERRITE-MARTENSITE STEELS

A Report Submitted
in Partial Fulfilment of the Requirements
for the Degree of
MASTER OF TECHNOLOGY

By
BIMAL KUMAR JHA

to the

DEPARTMENT OF METALLURGICAL ENGINEERING
INDIAN INSTITUTE OF TECHNOLOGY, KANPUR

MAY, 1980

CERTIFICATE

This is to certify that the thesis entitled "Deformation Characteristics of duplex Ferrite-Martensite Steels" by Bimal Kumar Jha is the record of work carried out under my supervision and has not been submitted elsewhere for a degree.

(R.K. Ray)
Assistant Professor
Department of Metallurgical Engineering
Indian Institute of Technology
Kanpur

April, 1980.

ACKNOWLEDGEMENTS

I take this opportunity to express my deep and profound sense of gratitude to Dr. R.K. Ray for suggesting this topic and for his inspiring guidance and encouragement at all stages of this work.

I am deeply indebted to my friends Mr. J.C.Nathani and Mr..A.K. Shah for their help at various stages of the work and without whom my stay here would not have been as enjoyable as it was.

Special thanks are due to Mr. Imran Ahmad, Mr. Ashwini Kumar and Mr. V.S. Verma for their time to time help in the work.

Finally, I thank Mr. K.N. Tewari and Mr. V.P.Gupta for typing the thesis and tracing the figures.

B Jha.

Bimal Kumar Jha

CONTENTS

SYNOPSIS

In the present investigation, the deformation characteristics of three Fe-Mn-Si-C dual-phase steels have been studied. For this purpose the alloys were given different heat-treatment schedules to attain different strength levels and microstructures. The Y.S., U.T.S., Uniform and total Elongation (%) values and the strain-hardening exponent 'n' were calculated from the experimental stress-strain curves of tensile tests. The microstructural aspects of the alloys were studied by both optical and electron microscopy.

The results of this investigation show that whereas dual-phase microstructure could be developed in a 0.1% C - 1.5% Mn alloy as well as a 0.1% C - 1.5% Mn - 1.5% Si alloy, the alloy with 0.1% C - 1.5% Si, was almost fully ferritic. The mechanical properties developed in the alloys with dual-phase structures were much superior to that of the alloy containing ferrite only.

A few theoretical models have been used to explain the strength of the dual-phase steels. The agreement between theory and practice was found to be quite satisfactory.

CHAPTER 1

INTRODUCTION

The "energy crisis" has stimulated the automobile industry to increase car gas mileage. One method would be to reduce the weight of the automobile. A direct approach to automotive weight reduction is reducing vehicle size. Further weight reduction may be attained by material substitution with plastics, aluminium or higher strength steels as replacements for plain carbon steel. Unlike plastics and aluminium, high strength steels have the same density as plain carbon steel but weight can be reduced by using thinner sections to carry the same load. Substitutions with high strength steels will usually require less modification of existing manufacturing process and equipment than substitutions of plastic or aluminium.

The formability of most high strength steels, e.g., renitrogenized steel and SAE980X and 950X high strength low alloy steel is poor compared to plain carbon steel. Only simple shapes can be formed and this has limited the widespread use of these steels in automotive applications. Recently developed dual phase HSLA-steels have attracted great interest because they offer very good combinations of strength and ductility. These properties make them

interesting to apply where increased strength is required to save weight and where a very good formability is required at the same time.

The dual-phase steels have typical microstructure consisting of about 80% polygonal ferrite and about 20% martensite. This microstructure is usually obtained in a continuous annealing line where the hot-rolled or cold-rolled strip is annealed high in the austenite/ferrite range and then air-colled. The properties of the vandium alloyed dual-phase steel VAN-QN may serve as an illustration of properties characteristics of the new group of steels, UTS $\simeq$ 650 MPa, total elongation $\simeq$ 28%. A conventionally treated HSLA steel of the same UTS would be expected to have a total elongation of only 20%, whereas its yield strength should be about 550 MPa as compared to about 400 MPa in the dual-phase steel. However, the dual-phase steel is characterised by continuous yielding and a large strain hardening in particular at low strains. Therefore, the yield strength in cold formed components will after the forming operation reach levels comparable to those of the conventionally treated HSLA-steel.

The objective of the present work is to critically survey factors controlling the structure and mechanical properties of a few dual-phase steels made in India.

CHAPTER 2

LITERATURE REVIEW

Low carbon steels processed to replace pearlite by martensite exhibit a decrease in yield strength, an absence of discontinuous yielding, and an increase in ultimate tensile strength when compared to the same steels prepared with a ferrite-pearlite microstructures[1]. Generally, the desirable mixture of ferrite and other phases is produced by intercritical annealing, i.e., heating between AC_1 and AC_3, and steels so treated have been identified as dual-phase steels. Although such materials have been studied for at least 10 years, it is only in the last three years that they have become of technological interest. It has been shown that, at a given tensite strength level, dual phase steels have superior formability to standard high strength low alloy steels[1-6].

Despite the name dual-phase, it is now recognized that a combination of three phases ferrite, martensite and retained austenite[1] may provide the best structure for applications where the good formability and strength of dual-phase steels are of considerable interest.

Below is given current dual phase processing routes and chemistries -

Table 2.1

Process	Approach	Chemistry	Status
As hot rolled	Climax[7] (lean)	0.05 Cmax, 1.1Mn, 1.0Si 0.4Mo, 0.5 Cr, 0.05Al.	Lab. exp.
	Climax (rich)	0.06 Cmax, 1.30Mn, 0.9Si, 0.4 Mo, 0.6 Cr.	Lab. exp.
	Dofasco (trial)	0.058 C, 1.62Mn, 0.5 Mo, 1.3 Si, 0.5 Cr.	Mill trial 2x10 ton coils
Continuous anneal	VAN QN[8] (VAN 80) (GM980X)	0.12C, 1.50 Mn, 0.5 Si, 0.02 N, 0.10 V.	Production
	Climax	0.11/0.12 C, 1.25/1.50Mn, 0.45/0.60 Si, 0.10/0.15Mo.	Lab. exp.
Bath aneal	U.S. Steel[9]	0.05 C, 3.00 Mn.	Lab. exp.
	Climax (Open, tight)	0.11 C, 2.2 Mn, 0.7 Si, 0.5 Mo, 1.5 Cr.	Lab. exp.

2.1 Deformation Models for Dual Phase Steels:

Reliable models for the description of the plastic deformation of two-phase materials is, of course, a very powerful tool in order to provide the metallurgist with guidelines for the alloying and heat treatment of dual-phase steels. A simple deformation model by Mileiko[10] has been made use of to examine which properties of the two constituents,

ferrite and martensite are most important to give the steel the best combination of properties. The main assumptions of this theory are:

(i) Equal strain in both phases.

(ii) The stress-strain relationship for the two phases obey $\sigma = K\varepsilon^n$.

Here σ = True stress

ε = True strain

K and n are constants.

Following Mileiko, the equations relating σ_c and ε_c, the tensile strength and true uniform strain of the dual phase steels, to the volume fraction V, of the martensite, given σ_m and σ_f, the tensile strength of martensite and ferrite respectively and ε_m and ε_f the true uniform strain of the martensite and ferrite respectively are as follows:

For uniform strain,

$$V = \frac{1}{1+\beta \frac{\varepsilon_c - \varepsilon_m}{\varepsilon_f - \varepsilon_c} \varepsilon_c \varepsilon_m - \varepsilon_f}$$

where

$$\beta = \frac{\sigma_m}{\sigma_f} \frac{\varepsilon_f^{\varepsilon_f}}{\varepsilon_m^{\varepsilon_m}} \frac{\exp \varepsilon_m}{\exp \varepsilon_f}$$

For tensile strength $\sigma_c = V \lambda' \sigma_m + (1-V) \lambda'' \sigma_f$

where $\lambda' = (\varepsilon_c/\varepsilon_m)^{\varepsilon_m} \exp(\varepsilon_m - \varepsilon_c)$

and $\lambda'' = (\varepsilon_c/\varepsilon_f)^{\varepsilon_f} \exp(\varepsilon_f - \varepsilon_c)$.

By applying realistic values of the parameters K and n for the ferrite and martensite and assuming that uniform strains of the two phases are independent of their tensile strengths, Davies has calculated the uniform elongation as a function of the tensile strength of the steel for various tensile strengths of the ferrite and the martensite. Typical results from such calculations are shown in Fig. 2.1[5]. The conclusion to be drawn from this is that at the desired strength of dual phase steel (true UTS 750 MPa).

(i) The uniform elongation of the steel increases with the UTS of the ferrite.

(ii) The uniform elongation of the steel increases with UTS of the martensite.

(iii) A larger increase in the uniform elongation is gained by increasing the strength of the ferrite than by increasing the strength of martensite at a strength level of 750 MPa of steel.

(i) and (ii) expresses the simple fact that the best properties of steel are reached for the best possible properties of the components. (iii) is a more significant result. since it can guide the metallurgist in the common situation where he has to make a choice between two possibilities which cannot be attained at the same time. In this context, it must be emphasized that the assumption made by Davies[6], that the uniform elongation of the phases

are independent of their strength is not always valid. In fact, it decreases, with some interesting exceptions, with increasing strength and consequently, even if the model as such is correct, the results may not be generally true.

However, as has been discussed by Öström and Hindgren[11] in the assumption of equal strain in the two phases is most certainly not fulfilled in the dual phase steels. Instead, there will be a partition of the strain, as well as of the stress, between the ferrite and martenite, such that the strain is considerably lower in the harder component than in the softer. Fig. 2.2[5] shows realistic partition of the strain and stress, and Fig. 2.3 shows the corresponding computed relationship between the uniform elongation and the UTS. Comparing with the results of the equal strain model gives, for equivalent properties of the components, that it is now more favourable to increase the martensite strength than the ferrite strength, hence opposite to the result obtained from the equal strain model. A further comparison of the two models showed that they both predict in agreement with experimental findings, a linear relationship between the tensile strength and volume fraction of martensite. Another model due to Araki et.al.[12] between the two phases produces a linear dependence. Hence, it seems that such a linear relationship is not sensitive to the model used. The predicted relationship for uniform

elongation and volume fraction of martensite may differ considerably between the models depending on the ratio between strength of martensite and ferrite[5]. Hence, the relationships are quite similar for relatively small differences between martensite and ferrite strength whereas it becomes significant when the differences grows as can be seen by comparing Figs. 2.1 and 2.3. Similarly, the predictions of the model by Araki et.al.[12] approaches those of the equal strain model as the ratio between the martensite and ferrite strength decreases. Thus it can be concluded that:

(i) To get the best possible combination of UTS and elongation for the dual-phase steel the best possible UTS and elongation of the ferrite and martensite must be used.

(ii) Depending on whether one gives more confidence to the equal strain or the strain partitioning model the UTS/elongation of the steel could be improved most either by increasing (percentage-wise) the strength of the ferrite or the martensite. Which way is most advantageous depends also on the strength level of the steel that is considered. It should, however, be born in mind that in practice more can often be done to the strength of the ferrite in dual-phase steel than to the strength of martensite; the strength of martensite is determined by the Carbon content and that tends to be about the same in mildly cooled dual phase steels.

Although these view points undoubtedly are of value in designing dual-phase steels it has to be recognized that many aspects of great importance for the properties are not contained in these models. For instance, as already pointed, the uniform elongation of ferrite and martensite are generally not independent of the UTS, an assumption used for the input data to the models. Furthermore, the models overlook entirely the distribution of the phases in the microstructure, clearly the number shape and size of the martensite will affect the properties of the steel significantly.

2.2 Metallurgy of Dual-Phase Steels

2.2.1 Strength: From a study of a series of Fe-Mn-C alloys[2] that were heat treated in the intercritical $\alpha + \gamma$ region and then quenched to give structure containing various amounts of martensite and martensite with different carbon contents, it was concluded that the strength is propertional to the percent martensite, Fig. 2.4. It appears that the strength is governed by a simple rule of mixtures between a strong martensite and weak ferrite. The strength appears to be independent of the carbon content in the martensite over the range studied (0.3 to 0.6 wt.% C) which is the composition region of practical interest, the reason for the strength of the dual-phase structure being independent of the martensite composition (strength) is not

known. However, it should not be concluded that the strength of a dual-phase steel is totally independent of the strength of second phase. Dual-phase steels in which the second phase is either zero-carbon martensite (low strength) or fine pearlite have a lower strength at comparable volume fractions of second phase[4,13].

The mechanical properties of the ferrite matrix, which, as will be shown, control the ductility of dual-phase steels, nevertheless influence the strength of these steels[6]. For optimum properties the ferrite should be very fine grained and strengthened by substitutional alloying additions such as Si, which have minimal effects on ductility.

2.2.2 Ductility: From a study of several series of alloys, it was concluded that dual phase steels could be treated as composite of two ductile phases [2,4,13]. The theory of such composites[10] predicts that the strength is given by a law of mixtures and that the ductility of the composite is sensitive to the strength and ductility of the matrix. Thus favourable strength-ductility combinations as indicated in Fig. 2.5 reflect favourable combinations of strength and ductility in each phase. In practice, the ferrite should be as strong as possible and have high ductility. In general, the higher the strength the lower is the ductility. However, in low interstitial content iron, the ductility is essentially independent of grain size, i.e. strength.

The intercritical heat treatment should ensure a "clean", low interstitial content ferrite; the interestial atoms will be segregated to the austenite regions.

Addition of substitutional solute atoms are beneficial to the dual-phase steel properties since they increase the strength propertionally more than they decrease ductility. It has been found that silicon additions do indeed improve the ductility at a given strength level in dual-phase steels[14].

In general, the excellent combination of strength and ductility shown by dual-phase steels (Fig. 2.5)[6] is a result of having a dispersion of strong martensite in a strong (very fine grained, substitutionally alloyed), ductile (low interstitial content) ferrite matrix.

2.2.3 Structure control: In order to produce dual phase steels with tensile strength levels from 60 to 150 Ksi, it is necessary to control the percentage of martensite in the structure. Different methods of production of dual phase steel as a consequence of available facilities, strongly influence the selection of the chemistry of the steels.

The easiest conceptual way to control the structure is to rapidly quench ($\geq 2000^{\circ}C$/sec.) the steel from the intercritical region[6]. Since most of austenite would be

transformed to martensite during the quench, quite lean alloys could be used. The percentage martensite in the structure could be controlled by the both the chemistry of the steel and the quench temperature. The chemistry of steel will depend to some extent upon the thickness of sheet being quenched, i.e. cooling rate of the steel; it should be possible to produce sheet thickness upto 0.10 inch, and of any strength from allys containing from 0.05 - 0.10% C and 0.4 - 0.9% Mn[6].

These lean alloys besides being relatively inexpensive, have a further advantage in that they should be readily weldable, as their composition is that of common low carbon steel. However due to low hardenability of these steels the heat affected zone around the weld will be of low strength. This could be a serious disadvantage for highly loaded weldments.

Most of dual-phase steels available today is produced in stainless steel or hot-dip galvanizing lines that have been modified so as to give a cooling rate $\geq 100^{o}C$/sec after the intercritical anneal. To obtain an essentially martensitic second phase, these alloys must have a reasonably high hardenability; since the intercritical anneal always leads to high carbon austenite, the hardenability of VAN-QN is provided by 1.4% Mn, 0.5% Si, and 0.1% V. For VAN-QN, it was found that there was less martensite in an air cooled

than in quenched specimen even after the lowest practical intercritical annealing treatment[3], the lower the temperature of annealing the higher will be the carbon content of austenite and the greater will be hardenability. The percentage martensite, and thus strength, in aircooled VAN-QN was essentially independent of intercritical annealing temperature[3]; temperature control is thus less critical in this type of alloy.

Changes in the strength of dual phase steels produced on facilities with relative slow and fixed cooling rates; can be achieved, in either of two ways. One way is to modify the carbon content in a VAN-QN type of chemistry; this assumes that a ce tain fraction of the austenite will be converted to martensite upon cooling. For example, a higher carbon content will lead to more austenite at the intercritical annealing temperature and more martensite would be obtained to give a higher strength dual-phase steel. This approach to modify the strength would be appreciable for low strength dual phase steels, but, due to the adverse effect of carbon on weldability, could lead to problems if high strength (high carbon) steels were used in critical welded applications. Since these steels are all of relatively high hardenability, they will have an advantage over plain carbon steels in producing a minimum of softening in the heat affected zone of welds.

The second way to control strength would be to modify the hardenability of the austenite by changing the amount and types of substitutional alloying elements present. The higher the hardenability of the austenite, the more martensite will be obtained in the final structure. However, if the hardenability is reduced in an attempt to produce low strength dual-phase steels, then the second phase obtained may be non-martensitic which can give less than optimum mechanical properties[13].

To study the influence of substitutional alloying additions on the properties of dual-phase steels, a series of alloys were prepared by vacuum melting[14]. The base composition of steel was 0.11% C, 1.4% Mn and 0.5% Si. and to this was added singly and in all combinations 0.1% V, 0.2% Mo. and 0.5% Cr. The steels were hot-rolled to sheet about 0.1 in. thick which was then intercritically annealed for 8 minutes, and aircooled at approximately 30°C/sec. Tensile specimens with a gauge length 2 inch long and 0.5 inch wide were cut from the sheet.

The influence of annealing temperature upon the tensile strength of these alloys, has been shown in Fig. 2.6. It shows that the strength is dependent upon the substitutional alloying elements present and essentially independent of annealing temperature from 760 to 800°C.

Metallographic examination of the specimens confirmed that higher strength were associated with higher martensite contents[6]. Thus apparently it has been possible to increase the hardenability of the austinite with further alloying additions.

2.2.4 Fatigue: The useful life of many components when tested under extreme conditions is governed by the fatigue response of the material. Since dual phase steels are relatively new materials, there is very little fatigue data available for these steels. However, a study has been made of prestrained VAN-QN (tensile strength 95 Ksi) in the fully reversed push-pull fatigue mode[15]. The major findings of this investigation are:

1) the cyclic stress-strain curve, strain life response and notch sensitivity are little affected by prestrains of upto 8% (maximum studied),

2) the strain-life behaviour of VAN-QN is equivalent to that of SAE950X at low strain amplitudes as shown in Fig. 2.7, while at high strain amplitudes it has the best fatigue resistance of the steels compared. The low strain, long life region is yield stress dominated (VAN-QN has a yield stress similar to that of SAE 950X), while high strength short life is ductility controlled (VAN-QN exhibits higher elongation than SAE 980X),

3) in the notched configuration where results are compared by means of the Neuber parameter $S(=\Delta\sigma\ \Delta\varepsilon\ E)^{\frac{1}{2}}$

where $\Delta\sigma$ and $\Delta\varepsilon$ are the stress and strain amplitudes respectively and E is the Young's modulus. It is found[6] that VAN-QN is equivalent to SAE980X. In practice many components contain stress-raisers, such as holes and sharp corners, and thus VAN-QN and SAE 980X steels appear to be equivalent for fatigue controlled applications.

2.3 Influence of Heat Treatment Parameters and Alloying Elements on the Microstructure:

2.3.1 Annealing temperature and cooling rate: Although the desired structure of ferrite and martensite can be produced by annealing at temperatures above A_3 it is in the production of dual-phase steels normally achieved by annealing in the austenite/ferrite range (intercritical annealing). Quenching does not give time for diffusion controlled transformations to take place. Accordingly quenching after an intercritical anneal produces volume fraction of polygonal ferrite and martensite according to the equilibrium between ferrite and austenite at the annealing temperature. This presupposes that all austenite is transformed to martensite is not entirely true since in many cases there is some retained austenite. From this follows that the volume fraction and the carbon content of the martensite increases gradually with decreasing annealing temperature for dual phase steels quenched after the intercritical anneal. However, with the exception of one or two

cases, dual phase steels are industrially produced with cooling rates approximately corresponding to air cooling after annealing. Under such cooling conditions, it is now well documented that the volume fractions of martensite is insensitive to the annealing temperature within the two-phase region for typical dual-phase steels. The reason for this behaviour is simply that these cooling rates are sufficiently slow for carbon to equilibrate during the transformation of austenite to polygonal ferrite. This gives a certain volume fraction of ferrite and austenite for each temperature during the cooling irrespective of which temperature, it is started. When the steel has been cooled to a sufficiently low temperature the austenite/ferrite essentially stops and on further cooling the remaining austenite transforms to martensite. As the cooling rate is raised there will gradually be a decrease of the amount of ferrite formed and correspondingly more martensite, and eventually for quenching one reaches the situation where the phase contents reflects the equilibrium conditions at the annealing temperature. Naturally the carbon content of the martensite is lowered at the same time for a given annealing temperature.

As the annealing temperature is raised above A_3 the situation is somewhat changed due to the fact that

nucleation of ferrite is now necessary for the transformation. The nucleation requires some under cooling and as a result the ferrite formation is retarded as compared to transformation after intercritical annealing Fig. 2.8[5]. As a further result of this the remaining austenite will at a given temperature contain less carbon compared to the situation after inter-critical annealing and exhibits therefore a larger tendency to transform to pearlite. In agreement with this VAN-QN has been found to form pearlite more easily when annealed above A_3 than below[16].

Hence ferrite is more readily formed after inter-critical annealing, as compared to annealing above A_3, and at the same time the pearlite transformation is impeded. In other words, the hardenability is lowered with respect to ferrite formation and enhanced with respect to pearlite transformation. Exactly such a combination of behaviour is particularly desirable for a steel that should be transformed to a mixture of ferrite and martensite, and it is suggested that this is reason why intercritical annealing is considered advantageous in the production of dual phase steels.

It has been demonstrated that the distribution of martensite pools in the ferrite is affected by annealing procedure[11]. Thus, after annealing in the intercritical range the martensite occurs as chains of islands along the

ferrite grain boundaries whereas after annealing above A_3 the martensite exists as more isolated particles in the ferrite grain boundaries as well as the ferrite grain interiors, a difference that may be conceived from difference in the transformation.

For general principles, it is to be expected that the ferrite grain size is increased with increasing annealing temperature, below as well as above A_3. However, it has been shown that for the very fine initial microstructure in the hot band, as for VAN-QN, this effect plays a minor role[11]. But for coarser initial structures the effect is significant[11].

The martensite pools actually contain retained austenite has been reported by several investigators[11,16]. However, it is only recently that the occurrance of this phase has been studied more quantitatively[16]. For steels oil quenched from varying temperatures, it was found that the content of retained austenite increase with temperature in the inter-critical range and decreased somewhat above A_3. This behaviour was understood on the basis of increasing amount of austenite at the temperature and carbon content. An additional effect was the decreasing size of the austenite pools with decreasing temperature which was proposed to stabilize the austenite strongly against martensite transformation. It was furthermore found that the retained austenite

was extremely stable on further cooling to low temperatures, whereas it is quite readily transformed to martensite during plastic deformation[5].

2.3.2 Initial microstructure: Although the annealing treatment to produce the dual phase structure refines the grain size of the ferrite, a fine initial structure ascertains a finer structure after the anneal[11]. In order to assure that pearlite formation is avoided, or more generally expressed that a sufficient hardenability is attained a complete dissolution of the cementite is essential during the anneal. With the short annealing time, desired in production, it is therefore, important to have an initial structure of fine cementite in order to get a short time for dissolution.

2.3.3 Alloying elements: A balanced amount of alloying elements for hardenability is essential in the dual-phase steels in order to get the correct mixture of ferrite and martensite. Generally it is to be expected that the same type of formula as used for indexing weldability can be used for judging the hardenability of dual phase steels, e.g.

$$E_c = C\% + \frac{Mn\%}{6} + \frac{Cr\% + Mo\% + V\%}{5} + \frac{Ni\% + Cu\%}{15}$$

Besides the elements in this expression 'Si' is considered to be important in creating the correct structure because of its tendency to retard cementite formation[17] and thereby probably also the pearlite formation. It is also added due to its solid solution hardening effect and it hardens the ferrite matrix.

Carbon may need a special comment with respect to its effect on hardenability in dual phase steels. Rather small difference in the nominal carbon, carbon content may have a large influence on the hardenability[11]. In the context, it is also relevant to compare the micro-alloying elements V , Nb and Ti since there is a special interest to utilize HSLA steels based on one of these elements to produce dual-phase steels. Comparative experiments have been made for these elements and have shown that it is only 'V'- steel that after annealing and aircool gives the characteristics of a dual phase, i.e. continuous yielding, large strain hardening rate and improved combination of UTS and elongation[18-20]. The others gave discontinuous yielding and properties corresponding to those of normalized or hot rolled HSLA steels; thus indicating that they contained a microstructure of ferrite and pearlite. The reason for this difference may be that 'V' as such gives a higher hardenability than Nb and Ti. However, very little is known of the true effect of these

latter two elements in this respect. However, it may be said that they will to a large extent, be precipitated before and during the annealing and can, therefore, not contribute much to hardenability. 'V' on the other hand, has a larger solubility and will therefore be in solution during the annealing and contributes for that reason in full extent to the hardenability. Because of this difference between 'V', on one hand and Nb and Ti on the other, it is possible to precipitate V after the anneal in a sufficiently fine form for it to give precipitation hardening. The Nb and Ti exists already during the anneal largely as coarse precipitates and can, therefore, not be precipitated in a fine form during cooling after the anneal. However, whether this fine precipitation actually occurs for the cooling rates used in production of V-dual-phase steels or whether it remains in solution is still not clear. The steels do contain some V(C,N) precipitates.

2.4 Influence of Structure on the Mechanical Properties:

The dual-phase steels are considered for application where a good combination of cold formability and strength is required. Consequently, the combination of total or uniform elongation and UTS is commonly used to grade these steels.

In the following, the various structural parameters that affect this combined property have been discussed.

2.4.1 Influence of martensite structure: In accordance with the simple model discussed earlier UTS increases linearly with the volume fraction of martensite[2]. At the same time, also in qualitative agreement with the models, the uniform elongation is lowered[2]. The linear dependence between UTS and content of martensite is expected provided the strength of martensite is constant. However, the martensite can be varied by varying the annealing temperature in specimens that have been quenched after the annealing. Consequently, the 'C' content increase with decrease in annealing temperature and would lead to a gradual increase of the martensite hardness. What this contradiction is due to, has not been clarified, but the following plausible explanation may be suggested[5]. The 'martensite' - islands contains a larger fraction of retained austenite at high carbon content and are therefore softer. Finally, in view of the scatter in the experimental results it could not be ruled that the experiments are compatible with an increase of martensite hardness as the martensite content declines. Despite this somewhat unclear situation it seems quite certain that an increase in strength of second phase has an impact on the steel properties as proposed by the deformation modes. It is the belief that it is the lower strength of

pearlite as compared to martensite that makes the UTS/elongation inferior in ferritic-pearlitic dual-phase steels to the UTS/elongation in ferritic martensitic dual-phase steels[21] (Fig. 2.9).

A seemingly interesting observation is that the product of UTS and elongation, which may be taken as a measure of goodness of the two properties remains approximately constant upto about 20% martensite and then declines with increasing martensite content (Fig.2.10)[22]. This has then lead to the conclusion that optimum properties can be achieved at about 20% martensite. The reason given to the change at 20% in ref. 22, is that above that level, the large martensite content accelerates void formation strongly such that the fibrous fracture supersedes necking and thereby impairs the total ductility. However, the behaviour of UTS x elongation vs. martensite content in Fig. 2.10 may in fact be a simple mathematical consequence of the approximate linear relationship between UTS and elongation (Fig. 2.9)[5] which results in a parabolic decline of UTS x elongation with increasing martensite content. In addition it is not clearly stated how the experiments are performed and accordingly it is difficult to judge what the carbon contents of the martensite in the various samples are.

Slightly better elongation at a constant UTS has been reached by annealing above A_3 as compared to annealing below[11]. As already pointed out this resulted in a change of martensite structure such that for the higher annealing temperature the martensite pools occurred rather isolated from each other whereas for low temperature they occurred as chains along the ferrite boundaries. It is quite likely that this is the cause of the difference in elongation. However, other causes could not be entirely excluded, e.g. a somewhat lower martensite content for higher annealing temperature.

The significance of the retained austenite in the dual phase steels with respect to their mechanical properties has not yet been clarified. However, since it has been shown to transform to martensite during straining of these steels, it seems quite likely that the concomitant hardness rise may increase the strain hardening rate to such an extent that UTS/elongation is improved. Hence this would be equivalent to the phenomena, responsible for the properties in the so called TRIP-steels.

It has been demonstrated that the strength of the dual phase steels increases if the aircooling after the anneal is interrupted at a lower temperature, say 400°C and quenched as compared to if it has been aircooled all

the way to room temperature[5]. Again the cause is unclear; larger auto-tempering or stabilization of the austenite, thus leading to larger amount of retained austenite, for the air cooled case may be possible explanation.

In a recent study[11] it was found that a carbon-Mn-V steel had better UTS/elongation than a C-Mn steel with the same composition except for 'V' after forced aircooling from 880°C (Fig. 2.11). The former steel contained 22% martensite and the latter 20% martensite plus 2% pearlite and accordingly the obvious reason for the different properties may be the absence of pearlite in the V-steel. However, at present it could not be excluded that V, beside raising the hardenability, has other effects.

As already discussed that with the exception of Carbon, other alloying elements have a minor influence on the mechanical properties of martensite, Carbon on the other hand increases its hardness strongly, but as discussed the expected effect of carbon have not been experimentally revealed.

2.4.2 Influence of ferrite structure: On the basis of the fact that the uniform elongation remains constant with decreasing grain size in pure ferrite, a fine ferrite grain size is considered to be favourable for the combination

of UTS and elongation in dual phase steels. However, minor grain size variation (3.8 - 7.3 micron) for the fine grain size typical of dual phase steels have proven to have no significant effect on the properties[11]. On the other hand, when quite coarse ferrite-martensite microstructures (50 - 100 micron) grain size are considered[23], it is found that they definitely exhibit inferior UTS/elongation than typical fine grained dual-phase steels.

Due to a larger rate of strain hardening solid solution hardening gives pure ferrite improved UTS/elongation to a larger extent than grain boundaries and precipitation hardening. The possibilities of utilizing substitutional alloying elements, Si and P have attracted great interest. Si, has because of its specially strong tendency to raise the rate of strain hardening, given very beneficial results in dual phase steels, as illustrated in Figures. 2.10 and 2.12. According to ref. 24, it is possible to improve the UTS/elongation by Mn just as much as by Si in pure ferrite and may be the effect of Mn in dual phase steels in this respect so far has been underrated. It should be noted that, according to results obtained for ferrite, the constancy of the n-value with varying grain size disappears when the steel is alloyed with Si and P, hence the advantage of a fine grain size may also be lost in dual

phase steels[5]. Perhaps this is the reason why no effect of a grain size variation 3.8 - 7.3 micron was observed in the C-Mn and C-Mn-V steels studied[11], after all, these steels contain significant amounts of Si and Mn($\simeq$0.7 and 1.4% respectively).

Precipitation hardening of ferrite is considered to affect the properties of dual phase steels unfavourably. However, this statement sterns entirely from ref. 24, where it was shown for ferrite that incoherent precipitates of TiC with a size of about 100 A^{o} had worse properties than solid solution hardening and grain boundary hardening. However, if for instance, 'V' occurs in the form of precipatates in V dual-phase steels they are likely to be fine and coherent and so far their effect on UTS/elongation is not known. In view of this uncertainty and in view of the fact that the state of 'V' in V dual-phase steels is not known precisely a final judgement of the role of precipitation hardening and of the exact role of elements like 'V', besides its role to increase hardenability and refine the grain size has to await further studies.

It is often stated that the ferrite in dual-phase steels should be clean, implying as it seems, that it should be free as possible of interstitials and precipitates. This is usually the motivation why mild cooling rates should

be preferred to quenching after annealing. However, this argumentation may be disputed since slow cooling rates may lead to low interstitial levels but does so by forming precipitates.

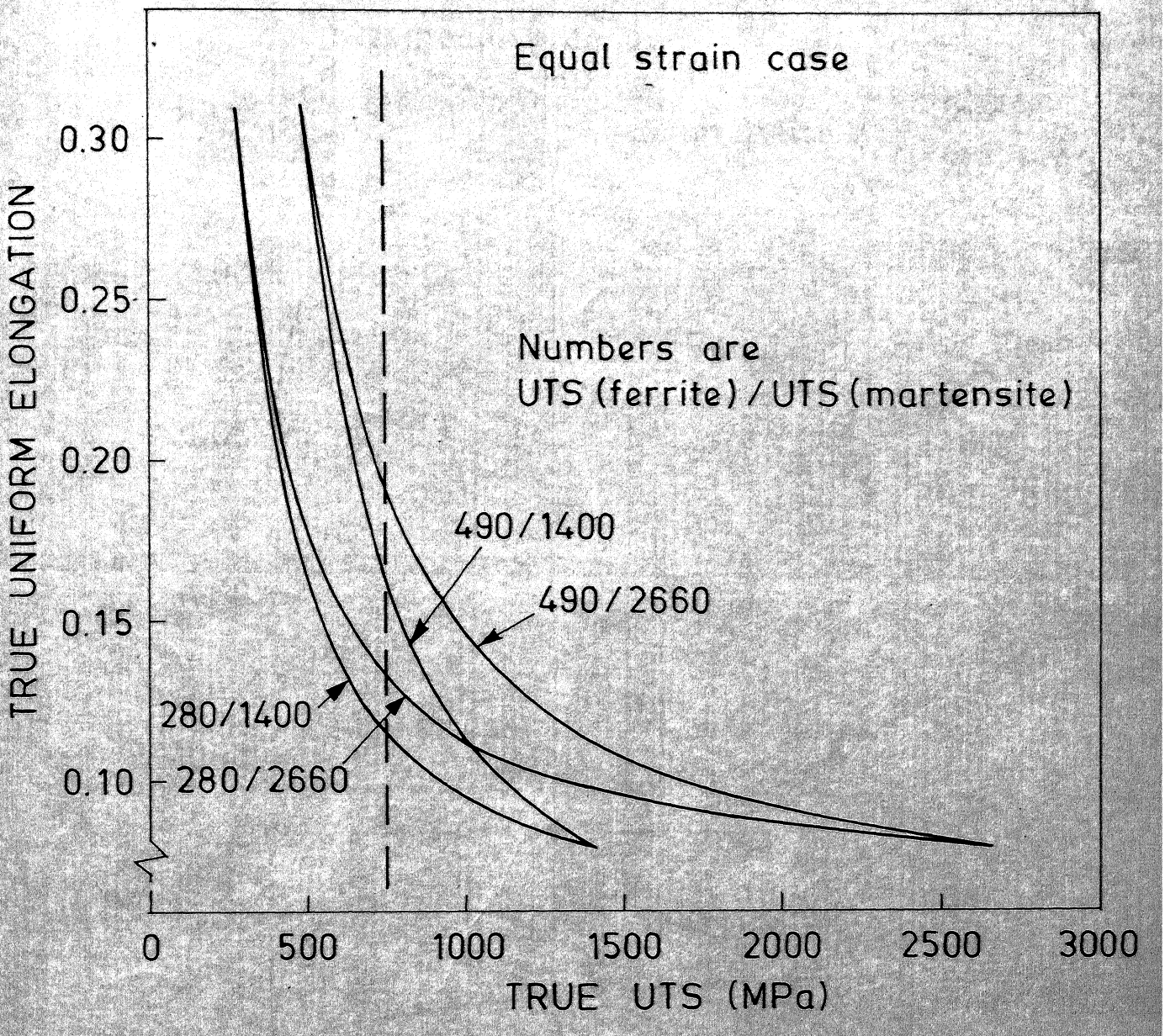

Fig. 2.1 Calculated curves of the uniform elongation as a function of the ultimate tensile strength for four composites. Equal strain case.

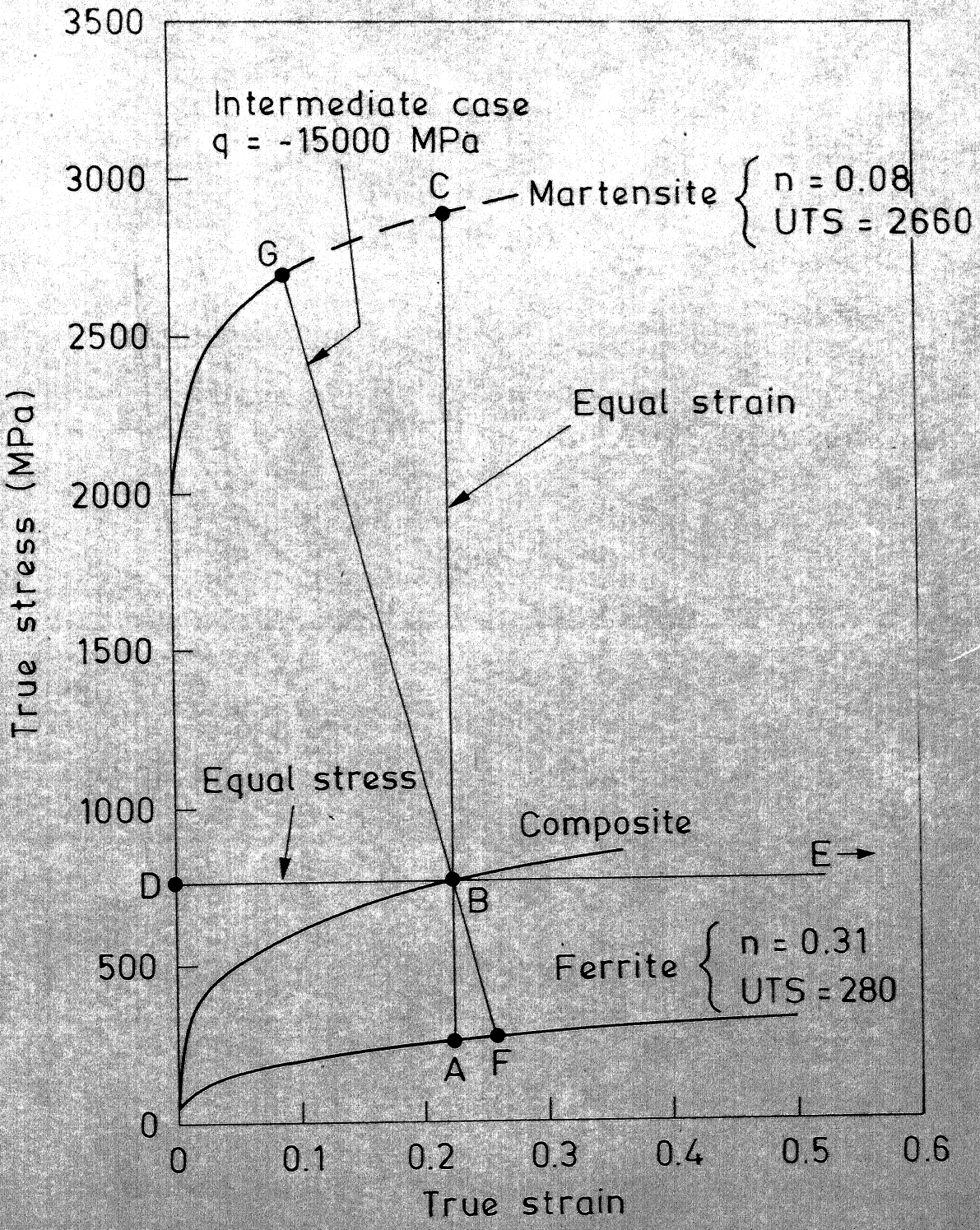

Fig. 2.2 Stress-strain curves of a ferrite, a martensite and a composite. The lines AC, FG and DE correspond to three different models. They connect the stress-strain states of the ferrite and the martensite which correspond to the stress-strain state B of the composite.

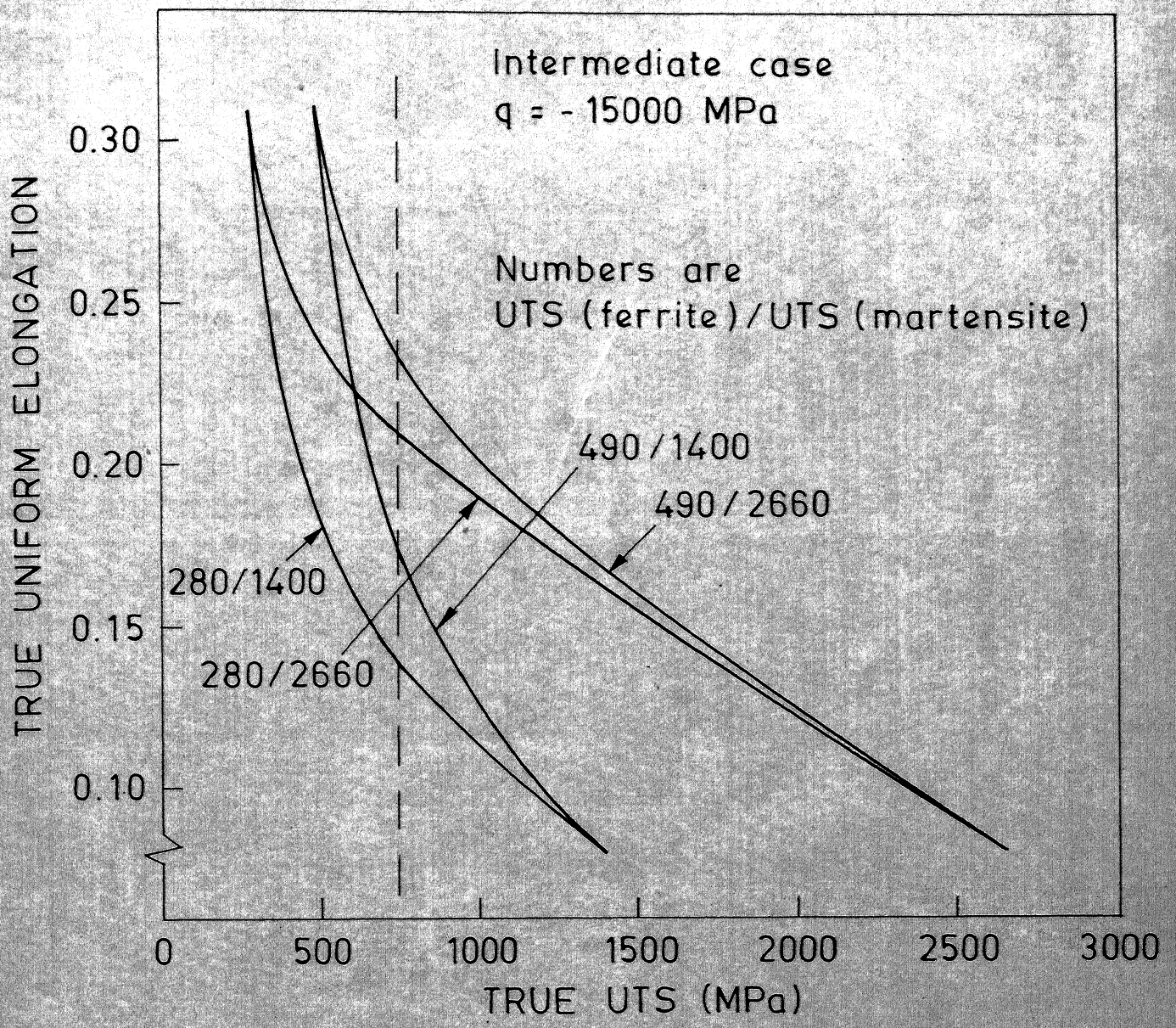

Fig. 2.3 Calculated curves of the uniform elongation as a function of the ultimate tensile strength for four composites. Intermediate case with q = - 15000 MPa.

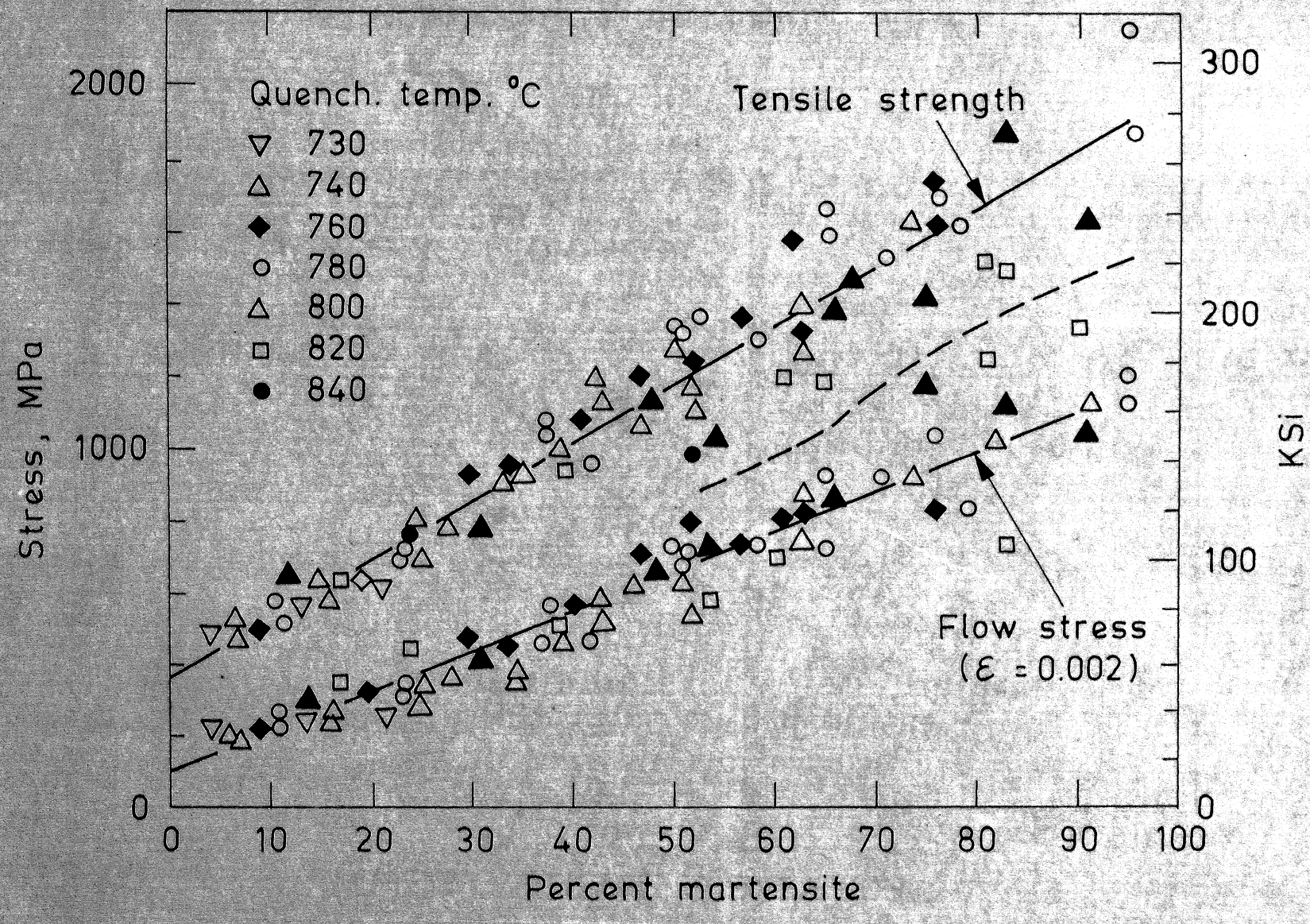

Fig. 2.4 The 0.2 pct. flow stress and the tensile strength as a function of percent martensite for a series of Fe-Mn-C alloys.

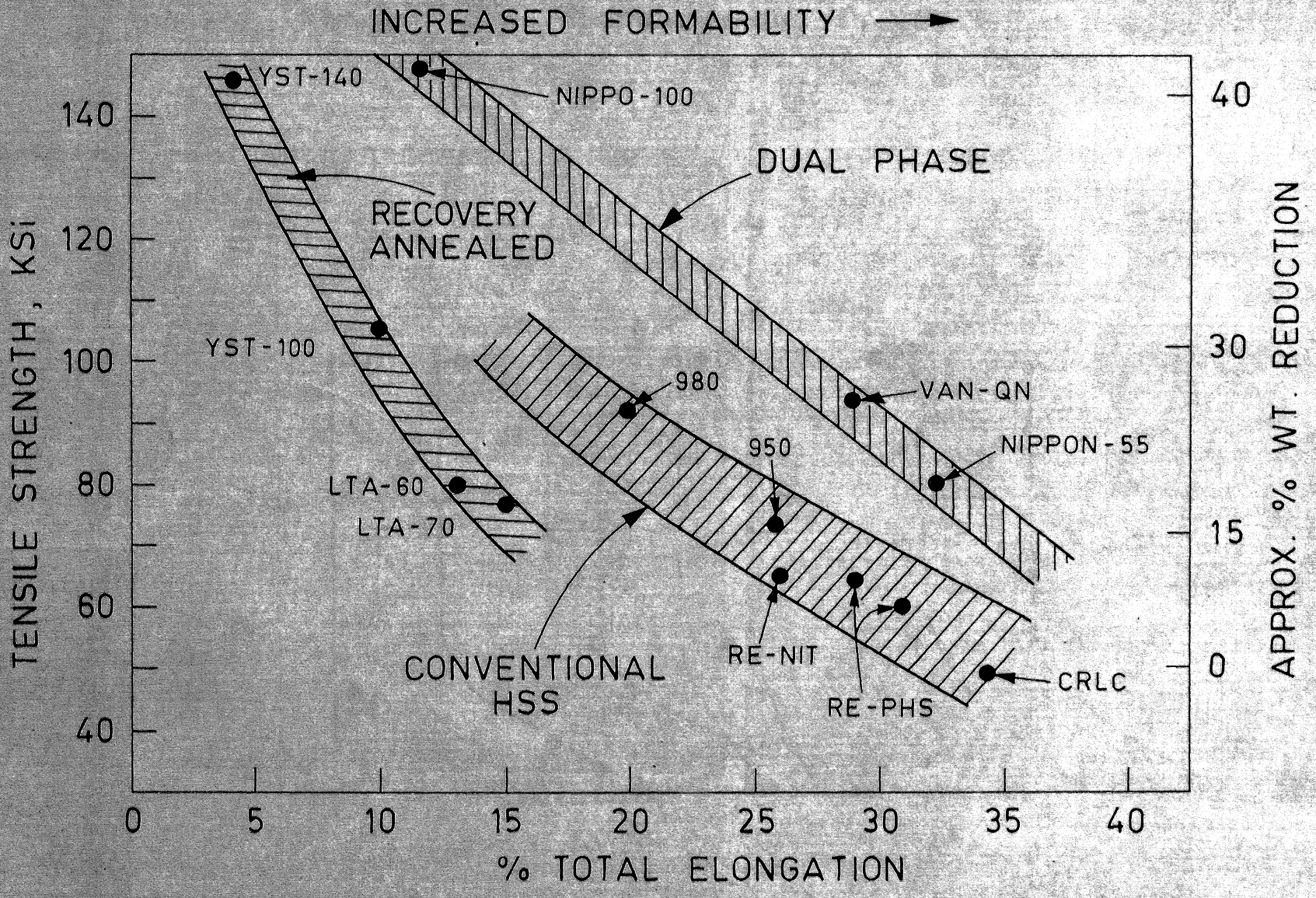

Fig. 2.5 Tensile strength as a function of percent total elongation for a few of the commercially available high strength steels; the approximate weight reduction was calculated with the assumption that fatigue resistance was the controlling factor.

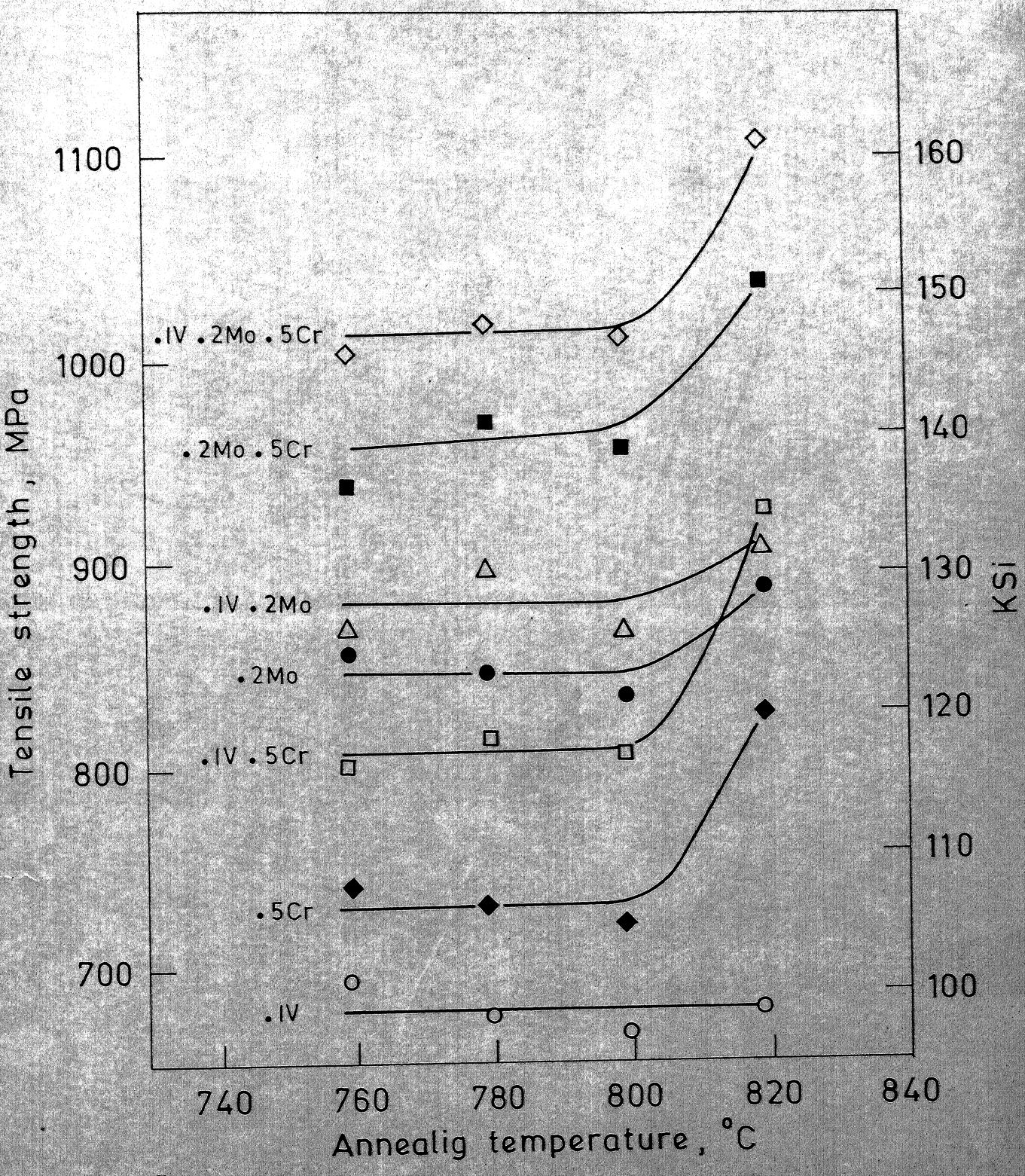

Fig. 2.6 The tensile strength as a function of intercritical annealing temperature for a series of dual-phase steels containing the indicated alloying additions.

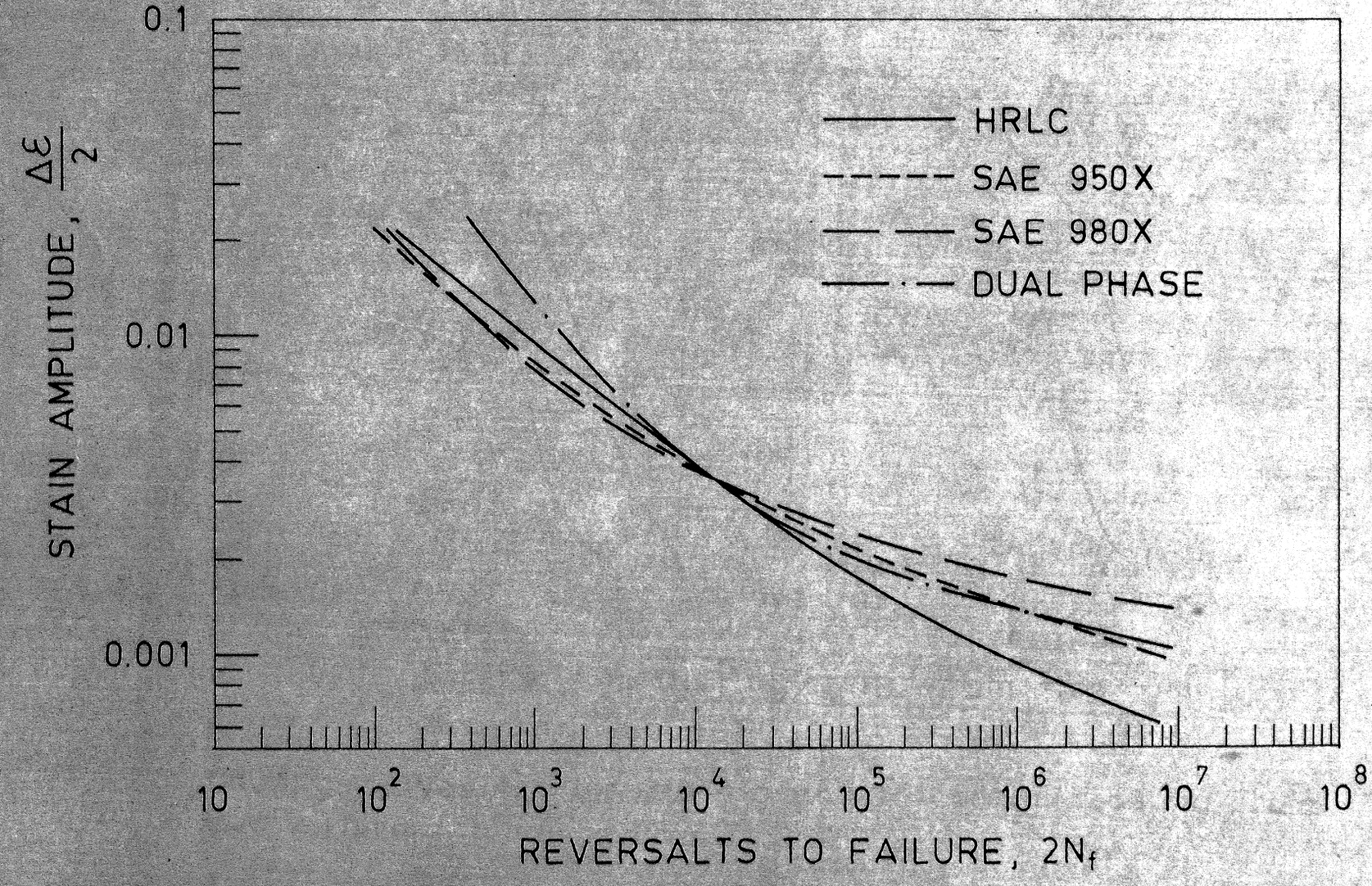

Fig. 2.7 Strain - life curves of four sheet steels.

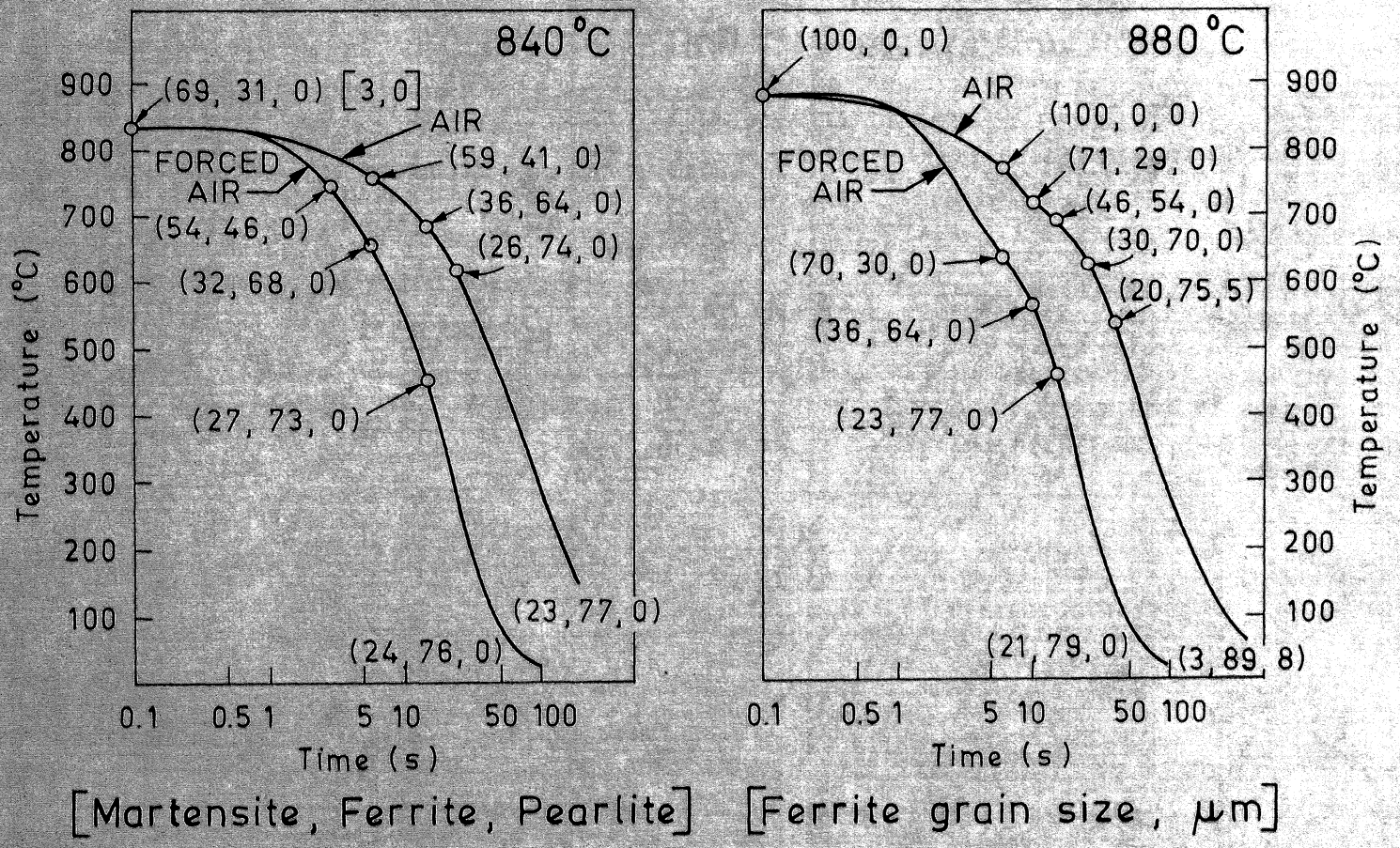

Fig. 2.8 Cooling curves for air cooling and forced air cooling from two different temperatures.

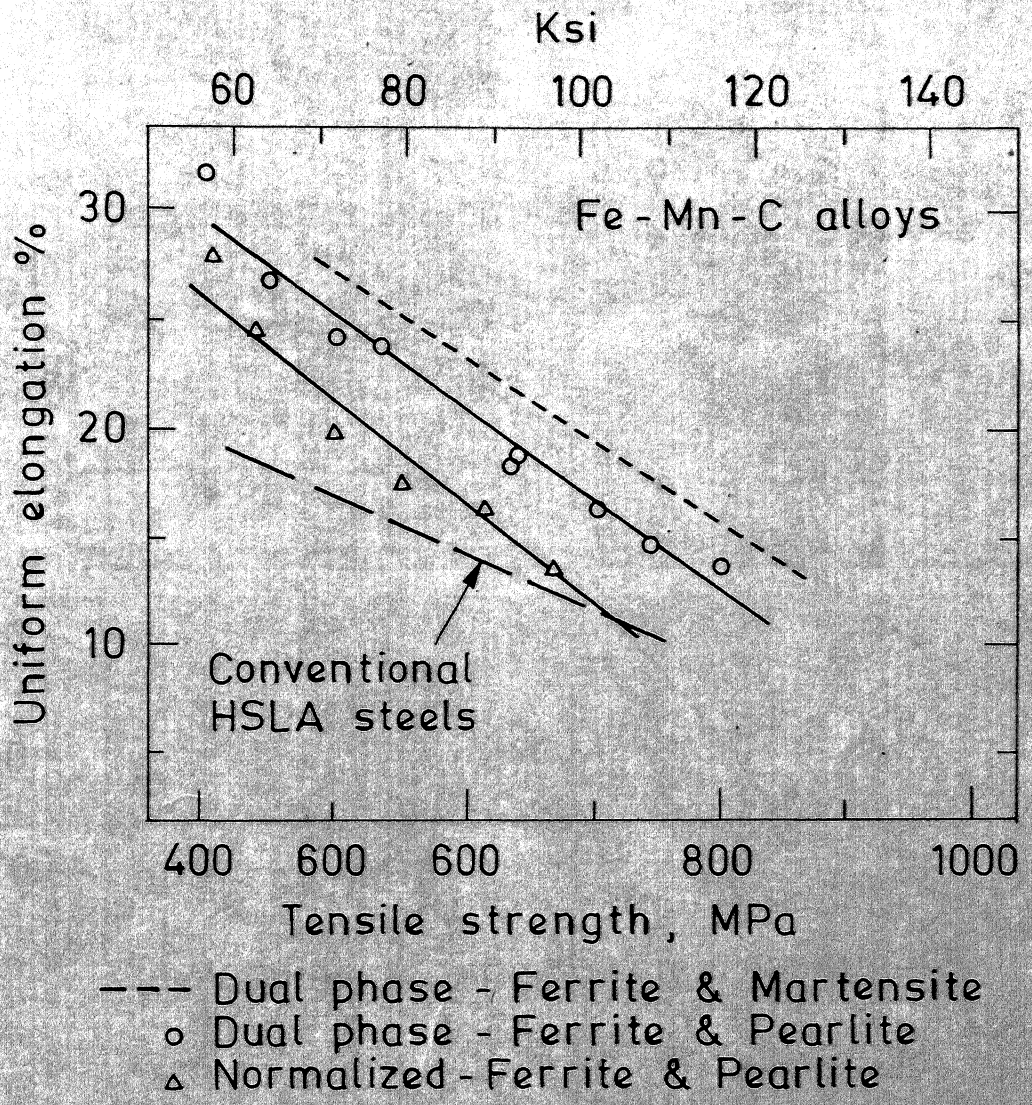

Fig. 2.9 Uniform elongation as a function of tensile strength for various Fe - Mn - C structures and conventional HSLA steels.

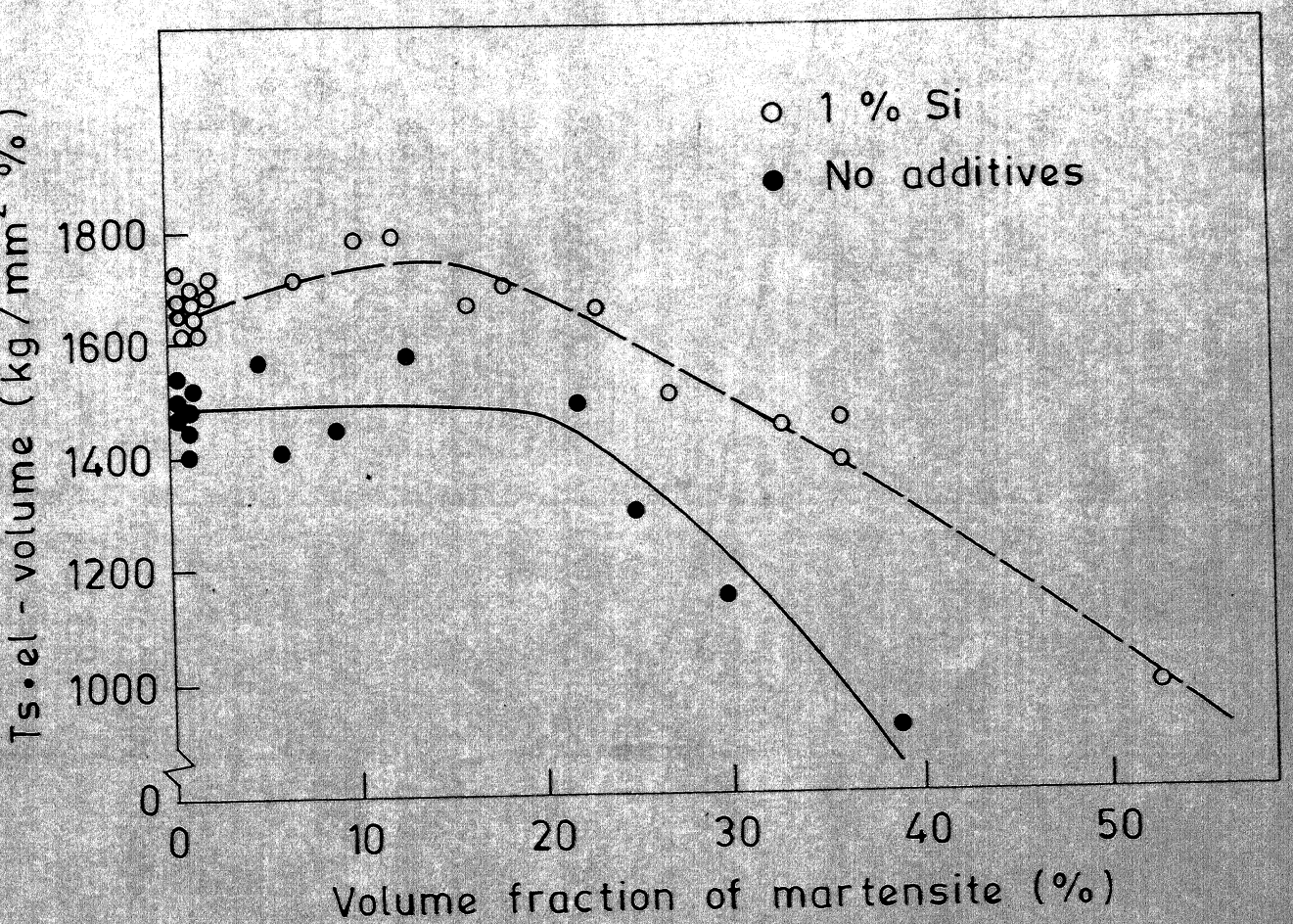

Fig. 2.10 UTS x elongation as a function of volume fraction of martensite for a dual-phase steel without and with 1 % Si.

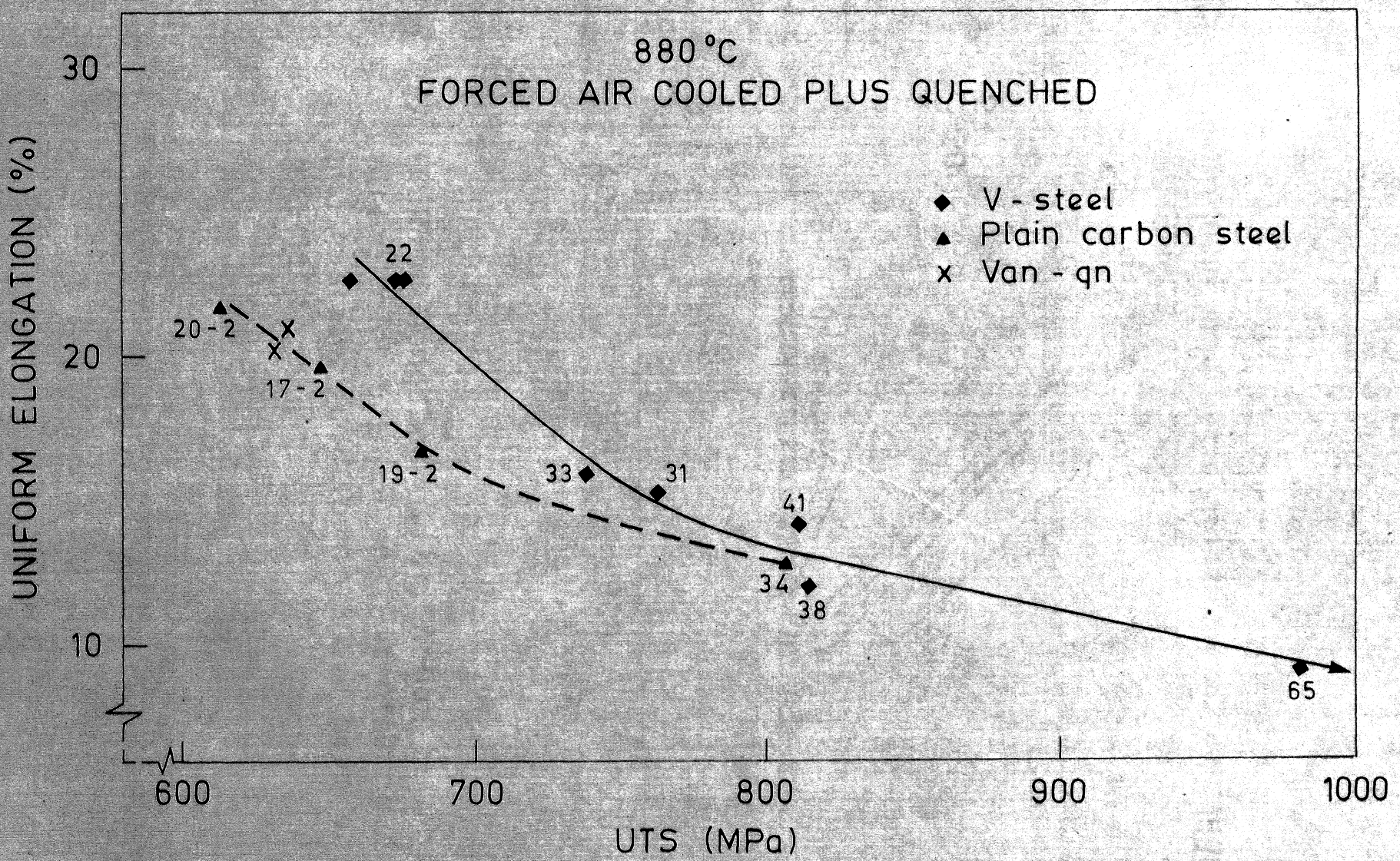

Fig. 2.11 Uniform elongation versus UTS for the V - steel and the plain carbon steel after annealing 10 minutes at 880 C and subscequent forced air cooling plus quenching. Single figures stand for the volume percent of martensite and double figures stand for the volume percent of martensite and the volume percent of pearlite.

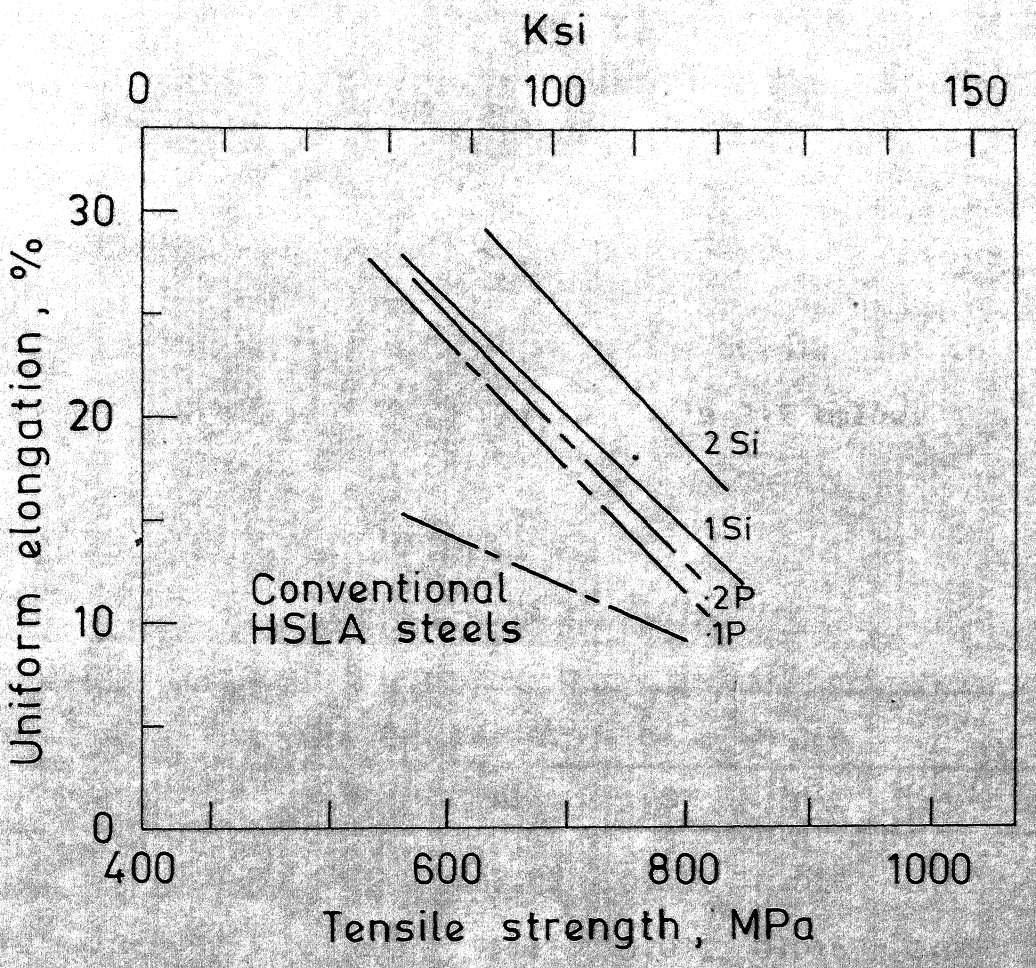

Fig. 2.12 Uniform elongation as a function of tensile strength for both Si and P containing dual-phase steels; data points have been omitted for clarity.

CHAPTER 3

EXPERIMENTAL PROCEDURE

3.1 Composition of Steels:

The chemical compositions of the steels used in the present investigation are shown in Table 3.1 below.

Table 3.1

Compositions of Steels

Alloy No.	Weight percentage of elements					
	C	Mn	Si	S	P	V
1	0.11	0.15	1.52	0.011	0.018	0.09
2	0.12	1.51	1.47	0.021	0.016	0.09
3	0.11	1.48	Trace	0.027	0.014	0.08

3.2 Melting and Preparation of Alloys:

The alloys were melted in the form of 30 Kg ingots in an induction furnace and cast into pre-heated cast-iron moulds. All the heats were deoxidised by Aluminium shots and misch-metal. The cross-sectional area of each ingot was 12 cm. x 12 cm. (approx.). All the ingots were initially forged into rods of square (25 mm. each side) and circular

25 mm. dia. cross-sections. The 25 mm. dia. round rods were finally forged down to 12 mm. dia. rounds.

From the forged 12 mm. rods specimens of 2.5 cms length were cut for optical metallographic studies. In addition, disc-shaped specimens with a thickness of 4 mm were cut for electron-microscopic observations. Tensile specimens with a guage-length of 28 mm were also prepared from the forged rods for tensile testing.

3.3 Heat-Treatment of Alloys:

All specimens for optical and electron metallography as well as for tensile testing were given the proper heat treatment to develop a dual-phase structure consisting of ferrite and martensite.

The heat-treatment was carried out in two stages: (i) austenitising and (ii) inter-critical annealing. Four different austenitising temperatures, namely, 880°C, 910°C, 940°C and 970°C were chosen for the purpose. Specimens for optical and electron metallography as well as tensile testing were austenitised for a period of 30 minutes at each of these temperatures and then air-cooled. These were then held at each of the four inter-critical annealing temperatures, namely, 750°C, 770°C, 790°C and 810°C for 30 minutes and then directly quenched in water.

3.4 Optical Metallography:

The optical metallography specimens were properly ground and polished. These were then etched in 5% Nital and examined under a light microscope. Photographs were taken from the etched surfaces at a magnification of 400X.

3.5 Electron Microscopy:

The specimens for electron microscopy were first polished mechanically followed by chemical polishing in a solution containing 50% HCl and 50% H_2O by volume. Final electro-polishing was done by the "window" technique using a solution consisting of 33% by volume of concentrated HNO_3, and 67% by volume of methanol. A stainless steel strip was used as the cathode. During electro-polishing, the temperature of the electrolyte was kept at $0^{\circ}C$ with the help of an ice-bath. The electron microscopy of the thin foils were carried out in a Philips EM 301 machine operated at 100 KV.

3.6 Tensile Testing:

Tensile testing of all the samples was carried out in an Instron 1195 machine using a cross-head movement speed of 0.5 mm per minute. From the charts 0.2% proof stress, ultimate tensile strength, percentage uniform elongation and percentage total elongation values were calculated.

3.7 Determination of Strain-Hardening Exponent 'n':

From the engineering stress-strain curves, true stress and true strain values at regular intervals were calculated. The strain-hardening exponent 'n' of the tensile samples for each heat-treatment was then determined by plotting $\ln\sigma$(true stress) values against $\ln\varepsilon$(true strain) values and finding out the slopes in each case.

3.8 Determination of Martensite Volume-Fraction:

The martensite volume-fraction of each heat-treated sample was determined from the optical photographs taken from their polished and etched surfaces by the usual point-counting method. An average of approximately 400 counts was taken in each case.

CHAPTER 4

EXPERIMENTAL RESULTS

4.1 Tensile Test Results:

The Y.S., U.T.S., uniform and total elongation (%) obtained in case of the Alloy 1 for different heat treatments are shown in a tabular form in Table 4.1. These results are also shown graphically in Figures 4.1 and 4.2. It is clear from Figure 4.1 that in this alloy both the Y.S. and the U.T.S. vary only slightly with either the austenitising temperature or the inter-critical annealing temperature. Figure 4.2 shows however, that both the uniform and total elongation of the alloy are very much functions of the austenitising temperatures. In fact lower is the austenitising temperature, higher are the values of both uniform and total elongation. Both uniform and total elongation values are found to decrease slightly with increasing inter-critical annealing temperatures.

Figure 4.3 shows the $\ln\sigma$ versus $\ln\varepsilon$ plot for the alloy 1 austenitised at 970°C and then held at four different inter-critical annealing temperatures. It is clear from this figure that 'n' does not remain constant throughout the deformation process. It has got a rather high value at lower strains and decrease with larger strains. At high strain levels, 'n' shows a much higher

Table 4.1

Tensile Test Results for Alloy 1

Heat treatment (°C)	Y.S. ($Kg./mm^2$)	U.T.S. ($Kg./mm^2$)	Uniform Elongation (%)	Total Elongation (%)
880+750	52	78	27	32
880+770	52	78	26.6	31.5
880+790	54	79	25	30.5
880+810	56	80	25	30
910+750	56	79	26	30.5
910+770	56	80	24.6	28.3
910+790	56	80	23.5	28.0
910+810	56	81	22	26.5
940+750	53	78	21.6	26.6
940+770	54	79	21.5	25
940+790	54	79	21	25
940+810	54	79	21	25
970+750	54	78	22	24.6
970+770	54	78	22	24.6
970+790	54	79	20.5	24
970+810	54	79	20	24

value (n = 0.28) for the material heat-treated at the lowest temperature of 750°C than at the other three higher temperatures (n values being $\simeq$ 0.10).

The tensile test results for Alloy 2 are shown in a tabular form in Table 4.2. These are again shown graphically in Figures 4.4 and 4.5. Figure 4.4 shows that both the Y.S. and U.T.S. of this alloy increase perceptibly with increase in the inter-critical annealing temperature, the austenitising temperature being kept fixed. For a particular intercritical annealing temperature the yield strength, in particular, shows a higher value for a lower austenitising temperature.

Figure 4.5 indicates that both the uniform and total elongation values show a downward trend with increasing inter-critical annealing temperature, the austenitising temperature being kept fixed. It can further be observed that at any particular inter-critical annealing temperature, the uniform and total elongation values are higher, lower the austenitising temperature.

From the $\ln \sigma$ versus $\ln \varepsilon$ plots for this alloy (Fig. 4.6) austenitised at 970°C and inter-critically annealed at four different temperatures, it is clear that the strain-hardening exponent 'n' does not remain constant during the whole process of deformation. It has much higher values at lower strain levels and goes on decreasing with

Table 4.2

Tensile Test Results for Alloy 2

Heat treatment (°C)	Y.S. ($Kg./mm^2$)	U.T.S. ($Kg./mm^2$)	Uniform elongation (%)	Total Elongation (%)
880+750	75	92	29.2	36
880+770	81	98	28.5	31.6
880+790	84	102	26	30.5
880+810	87	106	24	27
910+750	74	98	28.6	34.1
910+770	78	100	27.2	30.5
910+790	81	104	25.5	29.5
910+810	83	108	24	26.6
940+750	70	94	28.2	32.5
940+770	78	100	28	31.5
940+790	81	104	25	28
940+810	83	105	23	23.6
970+750	70	93	24	27.3
970+770	76	98	23.6	27.8
970+790	77	103	22.8	26
970+810	82	108	18.6	24.5

increasing strain. At very high strain 'n' values are found to show an increase with increasing inter-critical annealing temperature. For example, value of 'n' for 750°C is 0.275, value of 'n' for 770°C is 0.29, value of 'n' at 790°C is 0.28 etc.

The tensile test results for alloy 3 are given in a tabular form in Table 4.3. The salient features of these results are also shown graphically in Figures 4.7 and 4.8. The trends observed in these figures are very much similar to those for the alloy 2(Figures 4.4 and 4.5) with the exception that for a particular type of heat-treatment the values of Y.S., U.T.S., uniform and total elongation (%) etc. are a bit on the higher side in alloy 2 in comparison to Alloy 3.

The $\ln\sigma$ versus $\ln\varepsilon$ plot for the alloy 3 is shown in Figure 4.9. As in case of alloy 2, in this alloy also it was found that 'n' has got a very high value at lower strain levels and then decreases at higher strain levels. The value of 'n' at higher strain levels have been found to range between 0.2 to 0.3.

4.2 Martensite Volume Fraction Results:

During the course of the investigation it was observed that alloy 1 after all different heat-treatments was almost fully ferritic - the martensite being

Table 4.3

Tensile Test Results for Alloy 3

Heat Treatment (°C)	Y.S. ($Kg./mm^2$)	U.T.S. ($Kg./mm^2$)	Uniform Elongation (%)	Total Elongation (%)
880+750	55	85	27	30.5
880+770	58	87	23	26.8
880+790	60	90	25	25.5
880+810	64	92	19	22.3
910+750	55	83	27	32.2
910+770	57	87	23.6	26.5
910+790	59	90	20.5	24.8
910+810	62	92	18.3	20.5
940+750	55	81	26.6	32
940+770	58	84	23.3	26.0
940+790	60	88	21.6	24
940+810	64	90	16.6	18.2
970+750	54	80	23.0	29.3
970+770	57	82	20.8	26.3
970+790	59	84	20	26
970+810	60	84	18.3	22.5

practically absent. On the other hand, in both alloys 2 and 3, depending on the heat treatment, the microstructure was found to consist of ferrite and martensite of variable proportions.

Figure 4.10 shows the variation of the percentage of martensite with inter-critical annealing temperature for samples of alloy 2 which were previously austenitized at four different temperatures. As expected the amount of martensite increases rapidly with increasing inter-critical annealing temperature. It is further observed that a lower austenitising temperature leads to lesser amount of martensite in the final microstructure.

Figures 4.11 and 4.12 show graphically the variation of the mechanical properties for alloy 2 with martensite volume fraction. It is interesting to note that these plots are very similar to Figures 4.4. and 4.5 which show the variation of mechanical properties for the same alloy with the inter-critical annealing temperature.

Figure 4.13 shows the variation of volume fraction of martensite with the inter-critical annealing temperature for the alloy 3. The main features of this plot are essentially similar to the corresponding figure for alloy 2 (Figure 4.10). The only difference between the two is that whereas for alloy 2 martensite volume fraction shows a rather

steep rise with increasing inter-critical annealing temperature, the rise in martensite volume fraction is not that sharp in case of alloy 3. Not only that, the martensite volume fraction levels after different heat treatment schedules are found to be a bit lower in case of alloy 3 in comparison to alloy 2.

The variation of the mechanical properties of the alloy 3 with martensite volume fraction are shown in Figures 4.14 and 4.15. As mentioned in case of the alloy 2, here also, the variation of mechanical properties with martensite volume fraction follows the same pattern as the variation of mechanical properties with the inter-critical annealing temperature (Figures 4.7 and 4.8).

4.3 Results of Optical Microscopy:

The optical micrographs taken from the etched surfaces of samples of alloy 1, austenitised at 880°C and then heat-treated at the inter-critical annealing temperatures of 750°C, 770°C and 810°C are shown in Figures 4.16(a), (b) and (c). The microstructure in each case consists essentially of polygonal grains of ferrite. No martensitic area could be observed in samples of alloy 1 given different heat treatments. However, a close look at the microstructures shows that quite a few ferrite grain-boundaries are pretty thick. These may be the martensitic areas - but this could not be conclusively proved. Even

if these are martensitic areas, their volume fractions will be negligibly small to be of any significant effect.

Figures 4.17(a), (b), (c) and (d) show the optical micrographs of the alloy 2, initially austenitised at 970°C and then inter-critically annealed at 750°C, 770°C, 790°C and 810°C respectively. The microstructure in all these cases consitsof two-phases- the light-etching ferrite grains and the dark-etching martensitic regions. It is clear from this series of micrographs that the volume fraction of martensite increases with increasing the inter-critical annealing temperature.

Figures 4.18(a), (b), (c) show the optical micrographs of the alloy 2, initially austenitised at three different temperatures, namely, 880°C, 910°C, and 940°C respectively and then inter-critically annealed at the same temperature of 750°C. The volume fraction of martensite in each case are not very different. Not much difference in grain size discernible in these three micrographs. However, closer look will suggest a slight increase in grain-size with increasing austenitising temperature. The grain-size, however,increases drastically when the austenitising temperature is raised to 970°C (Figure 4.17(a)).

A series of optical micrographs showing the variation of the relative volume fraction of martensite with increasing

inter-critical annealing temperature for alloy 3 are shown in Figures 4.19(a) to (d). The features are very similar to those observed in case of alloy 2.

4.4 Results of Electron Microscopy:

In order to have a clear idea regarding the internal structure of both the ferritic and martensitic areas thin foils made from selected number of all three heat-treated alloys were examined under an electron microscope.

Figure 4.20(a) shows a collection of ferritic grains in the as-forged alloy 1. Although practically no martensitic area could be seen in the optical microstructures of the heat-treated alloy 1, transmission electron-microscopy has revealed the presence of small martensitic areas along with ferrite in a few places. This is shown in the electron microstructure of the alloy austenitised at 880°C and then inter-critically annealed at 770°C (Figure 4.20(b)). In one case some striations were also seen within the martensitic area which may be internal twins (Figure 4.20(c)).

Dual-phase structure is clearly found to be present in the electron microstructure of the alloy 2. A series of micrographs taken from foils made from samples of alloy 2 austenitised at 880°C and then inter-critically annealed at 770°C is shown in Figures 4.21(a,b,c). In Figure 4.21(a), thick martensitic regions are found lying adjacent to heavily

dislocated ferritic areas. That this martensite is heavily twinned and dislocated will be clear from Figs. 4.21(b) and (c).

Dual-phase structures consisting of ferrite and martensite areas can also be observed in case of alloy 3. Figure 4.22(a) shows the electron mic. structure of the alloy 3 austenitised at 970°C and then inter-critically annealed at 790°C. A large number of martensite laths can be seen in this micrograph together with some ferrite. The orientations of the martensitic and the ferritic areas are given in Figures 4.22(b) and (c) respectively.

Martensite in lath-form has been observed in a number of foils from alloy 3. This is shown typically in Figure 4.23(a). The ferritic areas adjacent to martensite regions in this alloy are highly dislocated as can be seen from Fig. 4.23(b).

FIGURE CAPTIONS (page 57 - 82)

4.1 Variation of Y.S. and U.T.S. with intercritical annealing temperature for alloy 1.

4.2 Variation of uniform and total elongation with intercritical annealing temperature for alloy 1.

4.3 Plot of $\ln \sigma$ (true stress) versus $\ln \varepsilon$ (true strain) for alloy 1.

4.4 Variation of Y.S. and U.T.S. with intercritical annealing temperature for alloy 2.

4.5 Variation of uniform and total elongation with intercritical annealing temperature for alloy 2.

4.6 Plot of $\ln \sigma$ (true stress) versus $\ln \varepsilon$ (true strain) for alloy 2.

4.7 Variation of Y.S. and U.T.S. with intercritical annealing temperature for alloy 3.

4.8 Variation of uniform and total elongation with intercritical annealing temperature for alloy 3.

4.9 Plot of $\ln \sigma$ (true stress) versus $\ln \varepsilon$ (true strain) for alloy 3.

4.10 Variation of percent martensite with intercritical annealing temperature for alloy 2.

4.11 Variation of Y.S. and U.T.S. with martensite percent for alloy 2.

4.12 Variation of uniform and total elongation with percent martensite for alloy 2.

4.13 Variation of percent martensite with intercritical annealing temperature for alloy 3.

4.14 Variation of Y.S. and U.T.S. with percent martensite for alloy 3.

4.15 Variation of uniform and total elongation with percent martensite for alloy 3.

4.16(a),(b) and (c) - Optical micrographs of alloy 1, austenitised at 880°C and then heat treated at intercritical annealing temperatures of 750°C, 770°C and 810°C respectively. Mag - 1000X.

4.17(a),(b),(c) and (d) - Optical micrographs of the alloy 2 initially austenitised at 970°C and then intercritically annealed at 750°C, 770°C, 790°C and 810°C respectively. Mag - 1000X.

4.18(a),(b) and (c) - Optical micrographs of the alloy 2 initially austenitised at three different temperatures namely, 880°C, 910°C and 940°C respectively and then intercritically annealed at the same temperature of 750°C. Mag - 1000X.

4.19(a),(b),(c) and (d) - Optical micrographs of alloy 3 initially austenitised at 970°C and then intercritically annealed at 750°C, 770°C, 790°C and 810°C respectively. Mag - 1000 X.

4.20(a) Transmission electron micrograph of alloy 1 in as forged condition. Mag - 30,000X.

4.20 (b) and (c) - Electron micrographs of alloy 1 initially austenitised at 880°C and then intercritically annealed at 770°C. For (b) mag - 51000X,

For (c) mag - 18900X.

4.21(a), (b) and (c) - Electron micrographs of alloy 2, initially austenitised at 880°C and then intercritically annealed at 770°C.

For (a) mag - 23400X, For (b) mag - 23400X,

For (c) mag - 30,000X.

4.22(a), (b) and (c) - Electron micrographsof alloy 3 initially austenitised at 970°C and then intercritically annealed at 790°C.

For (a) mag - 39000X, For (b) mag - 39000X, orientation of martensite,

For (c) mag - 39000X, orientation of ferrite.

4.23 (a) and (b) - Electron micrographsof alloy 3 initially austenitised at 970°C and then intercritically annealed at 790°C.

For (a) mag - 18900X, For (b) mag - 18900X.

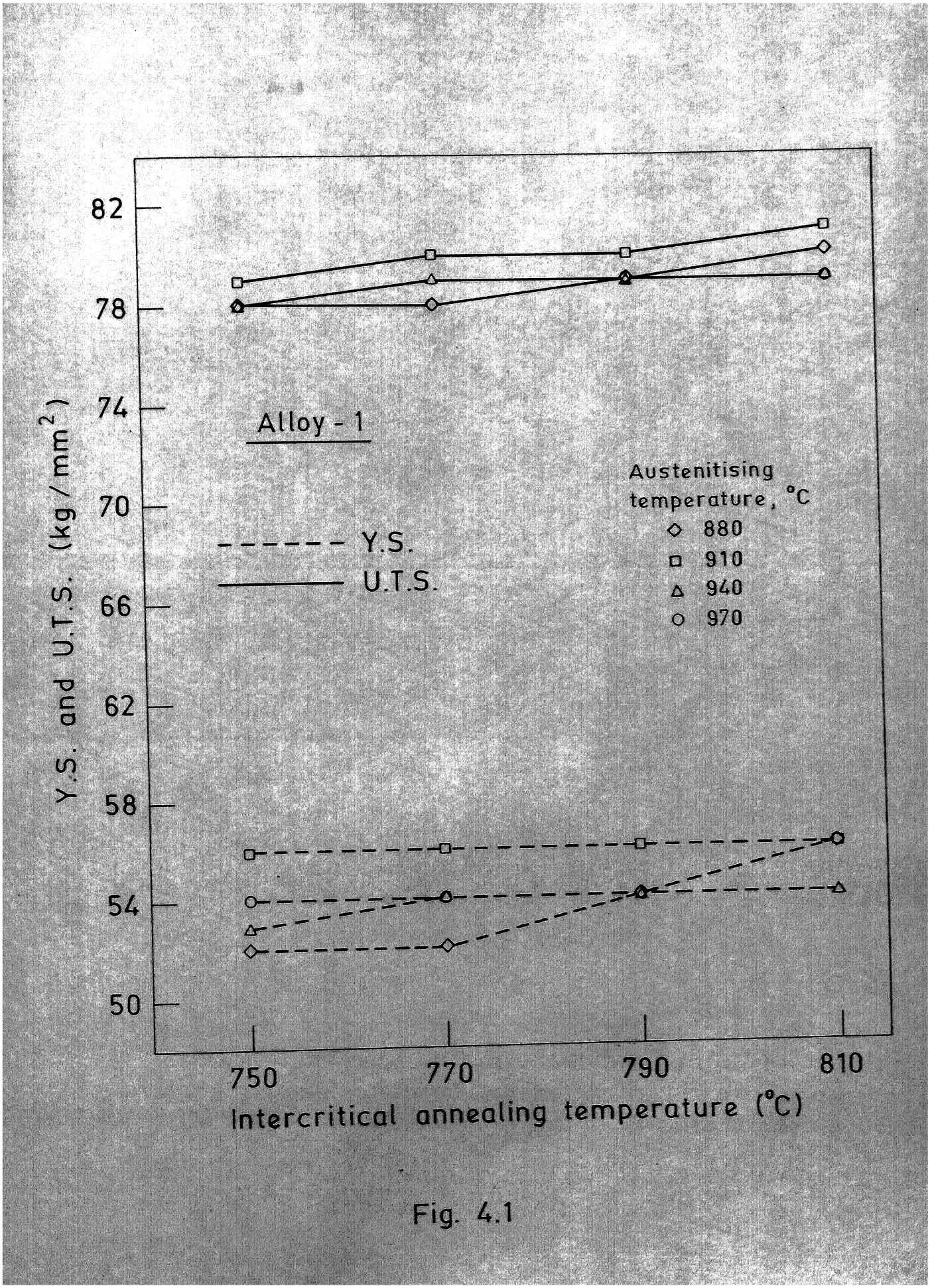
82
78
74
70
66
62
58
54
50
Y.S. and U.T.S. (kg/mm²)
Alloy - 1
Y.S.
U.T.S.
Austenitising temperature, °C
880
910
940
970
750
770
790
810
Intercritical annealing temperature (°C)

Fig. 4.1

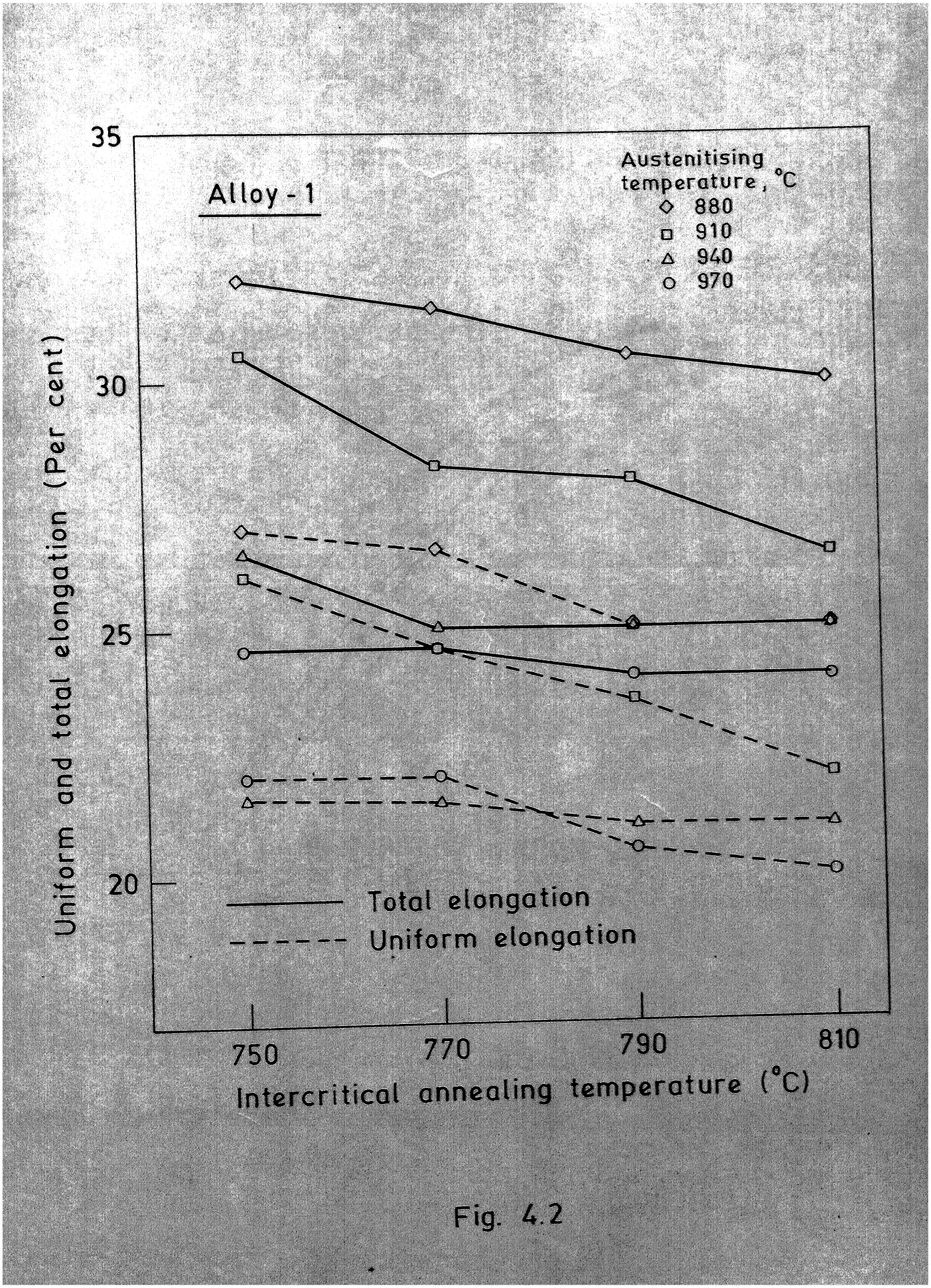
Alloy - 1
Austenitising temperature, °C
880
910
940
970
35
30
25
20
Uniform and total elongation (Per cent)
Total elongation
Uniform elongation
750
770
790
810
Intercritical annealing temperature (°C)

Fig. 4.2

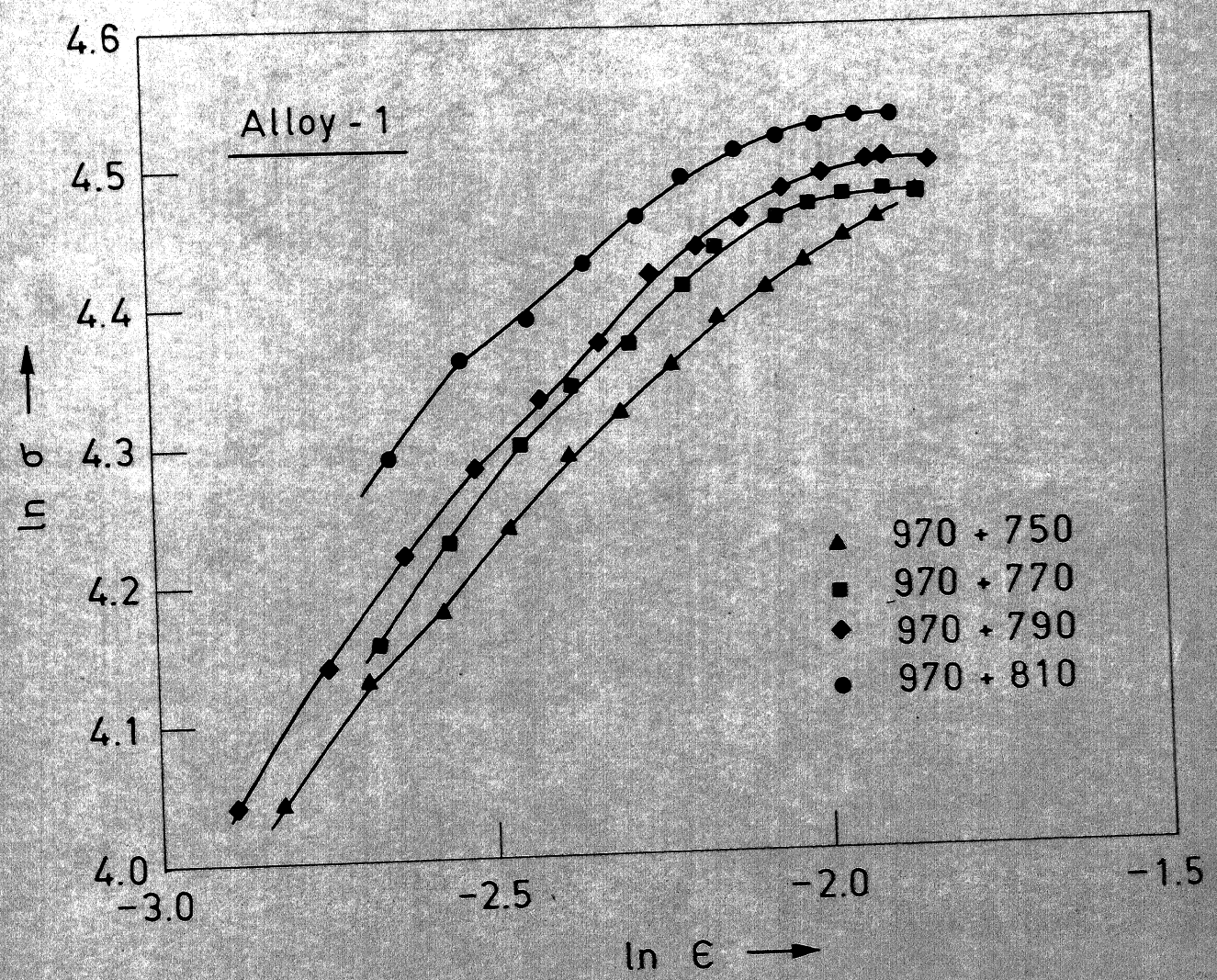
Alloy - 1
4.6
4.5
4.4
4.3
4.2
4.1
4.0
σ
−3.0
−2.5
−2.0
−1.5
ln ε
970 + 750
970 + 770
970 + 790
970 + 810

Fig. 4.3

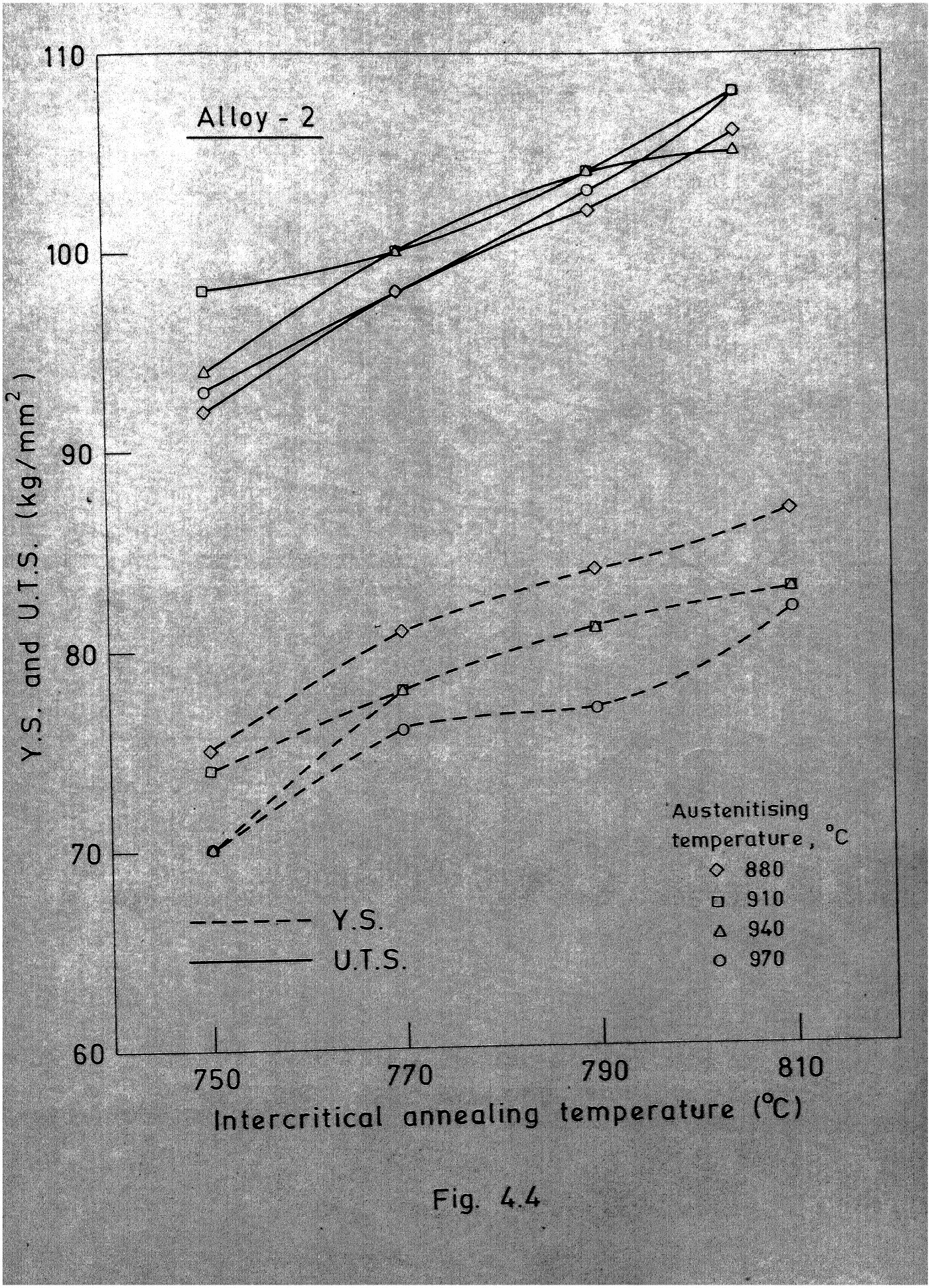
Alloy - 2
110
100
90
80
70
60
Y.S. and U.T.S. (kg/mm²)
750
770
790
810
Intercritical annealing temperature (°C)
Austenitising temperature, °C
880
910
940
970
Y.S.
U.T.S.

Fig. 4.4

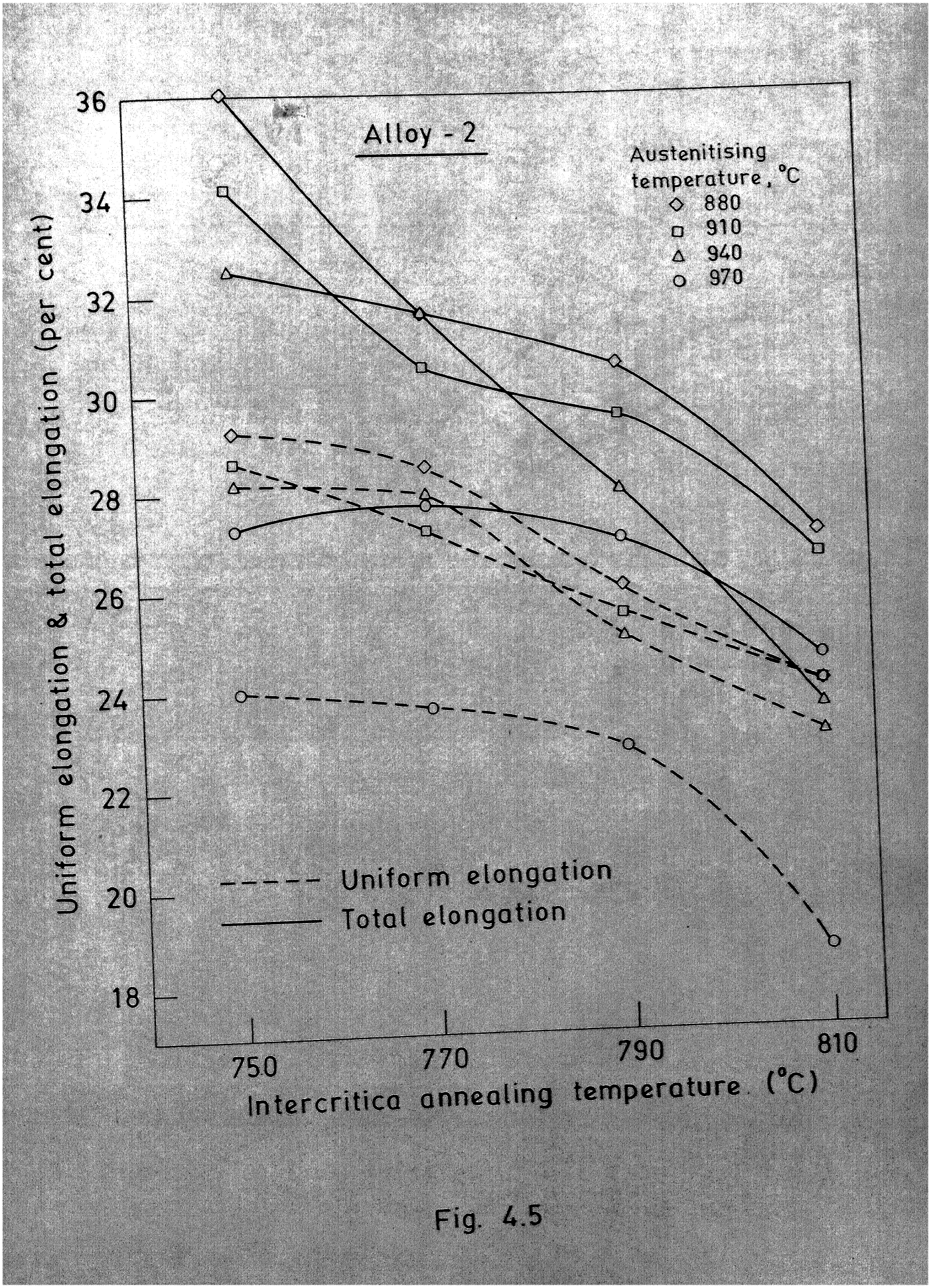
Alloy - 2
Austenitising temperature, °C
880
910
940
970
Uniform elongation
Total elongation
Uniform elongation & total elongation (per cent)
36
34
32
30
28
26
24
22
20
18
750
770
790
810
Intercritica annealing temperature (°C)

Fig. 4.5

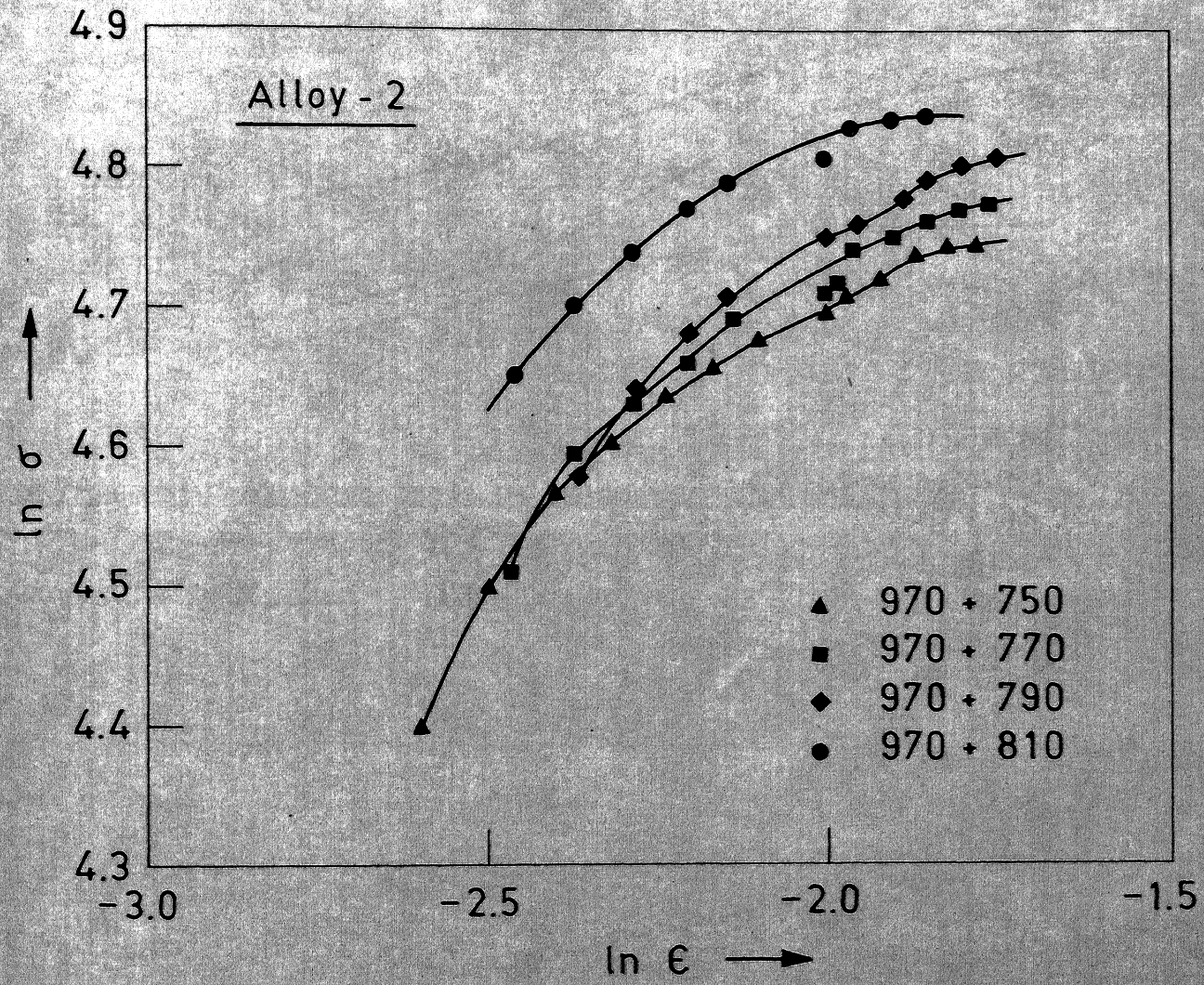
Alloy - 2
4.9
4.8
4.7
4.6
4.5
4.4
4.3
σ
-3.0
-2.5
-2.0
-1.5
ln ε
970 + 750
970 + 770
970 + 790
970 + 810

Fig. 4.6

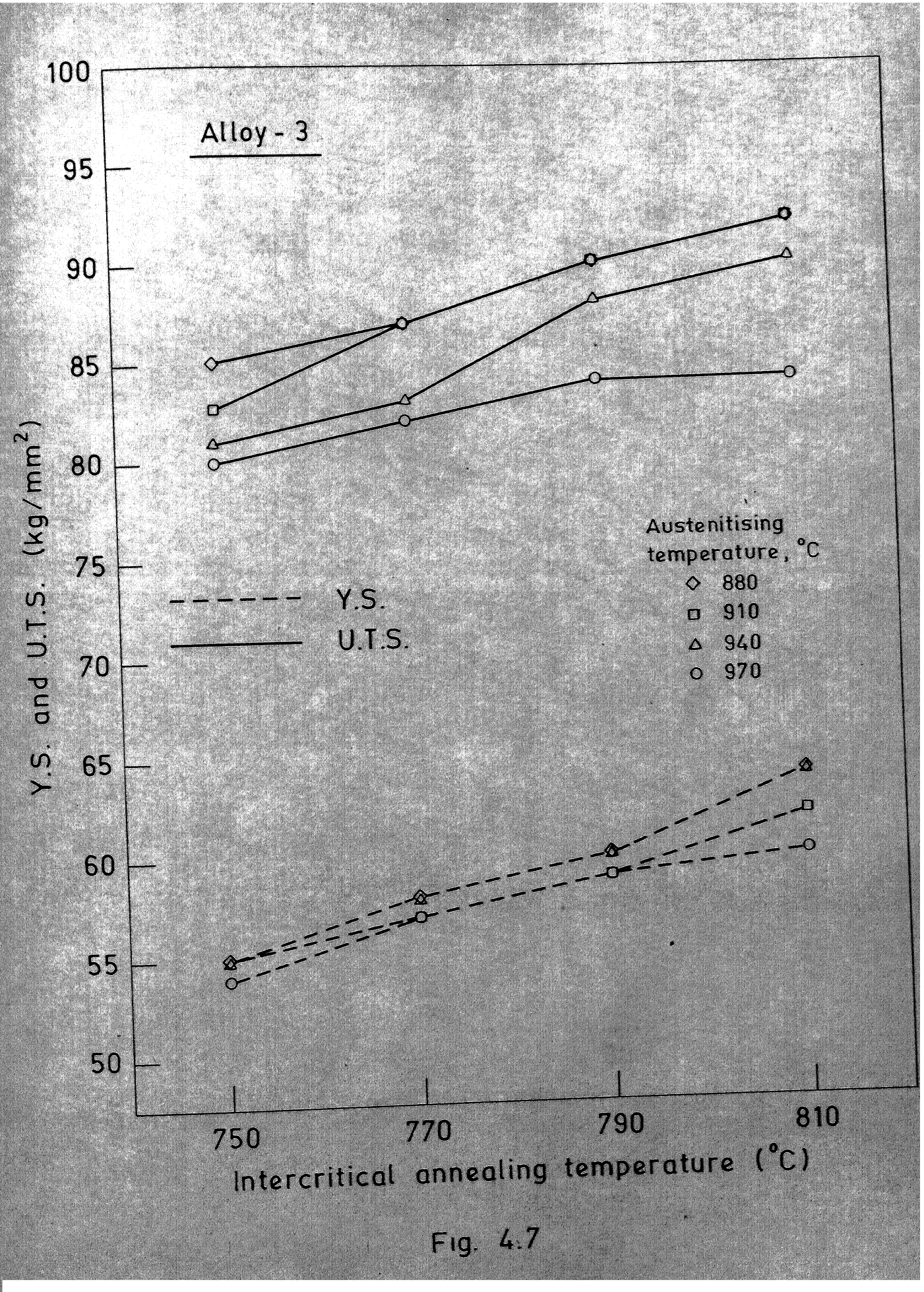
Alloy - 3
100
95
90
85
80
75
70
65
60
55
50
Y.S. and U.T.S. (kg/mm²)
Y.S.
U.T.S.
Austenitising temperature, °C
880
910
940
970
750
770
790
810
Intercritical annealing temperature (°C)

Fig. 4.7

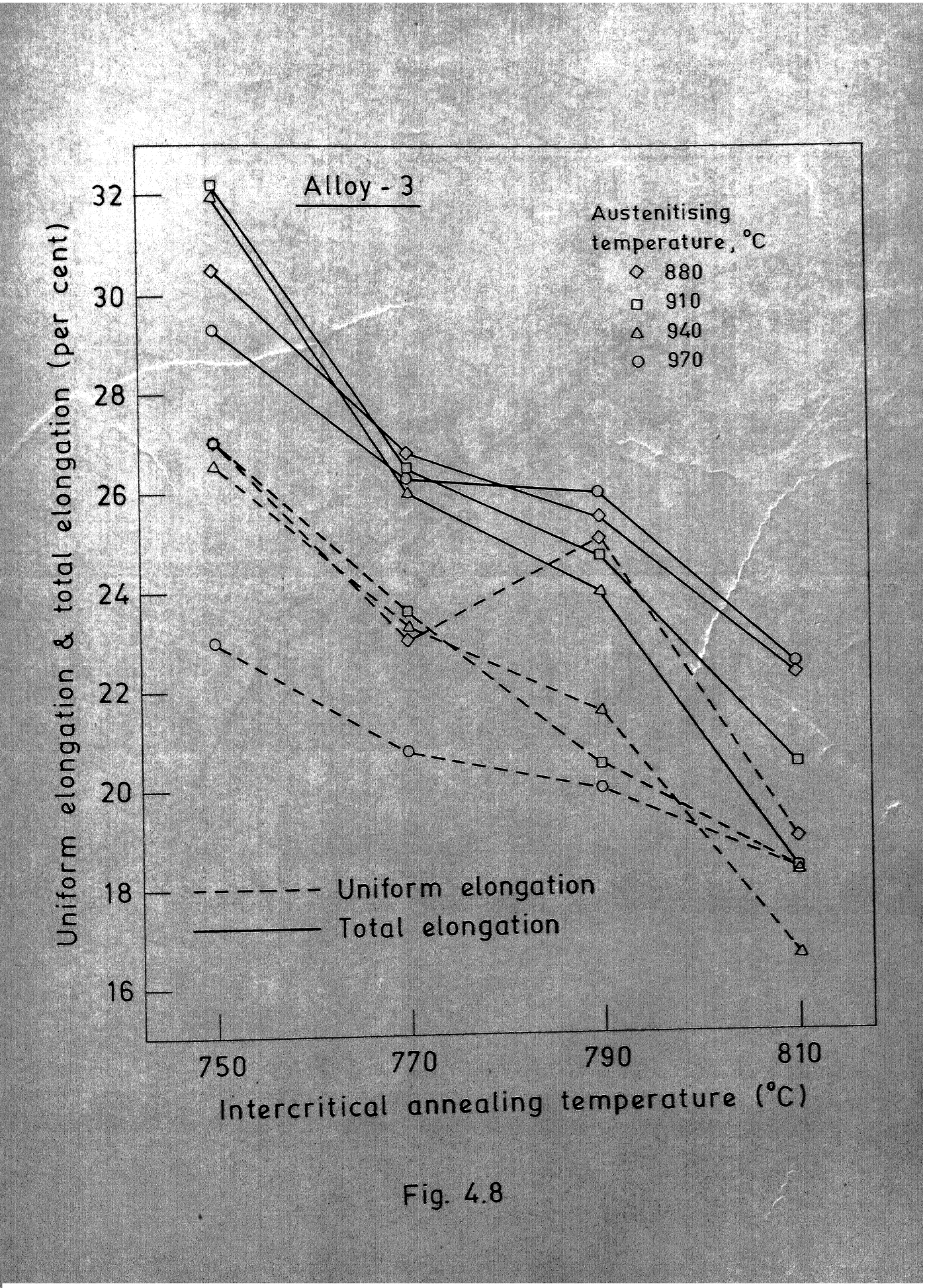
Alloy - 3
Austenitising temperature, °C
880
910
940
970
Uniform elongation
Total elongation
Uniform elongation & total elongation (per cent)
32
30
28
26
24
22
20
18
16
750
770
790
810
Intercritical annealing temperature (°C)

Fig. 4.8

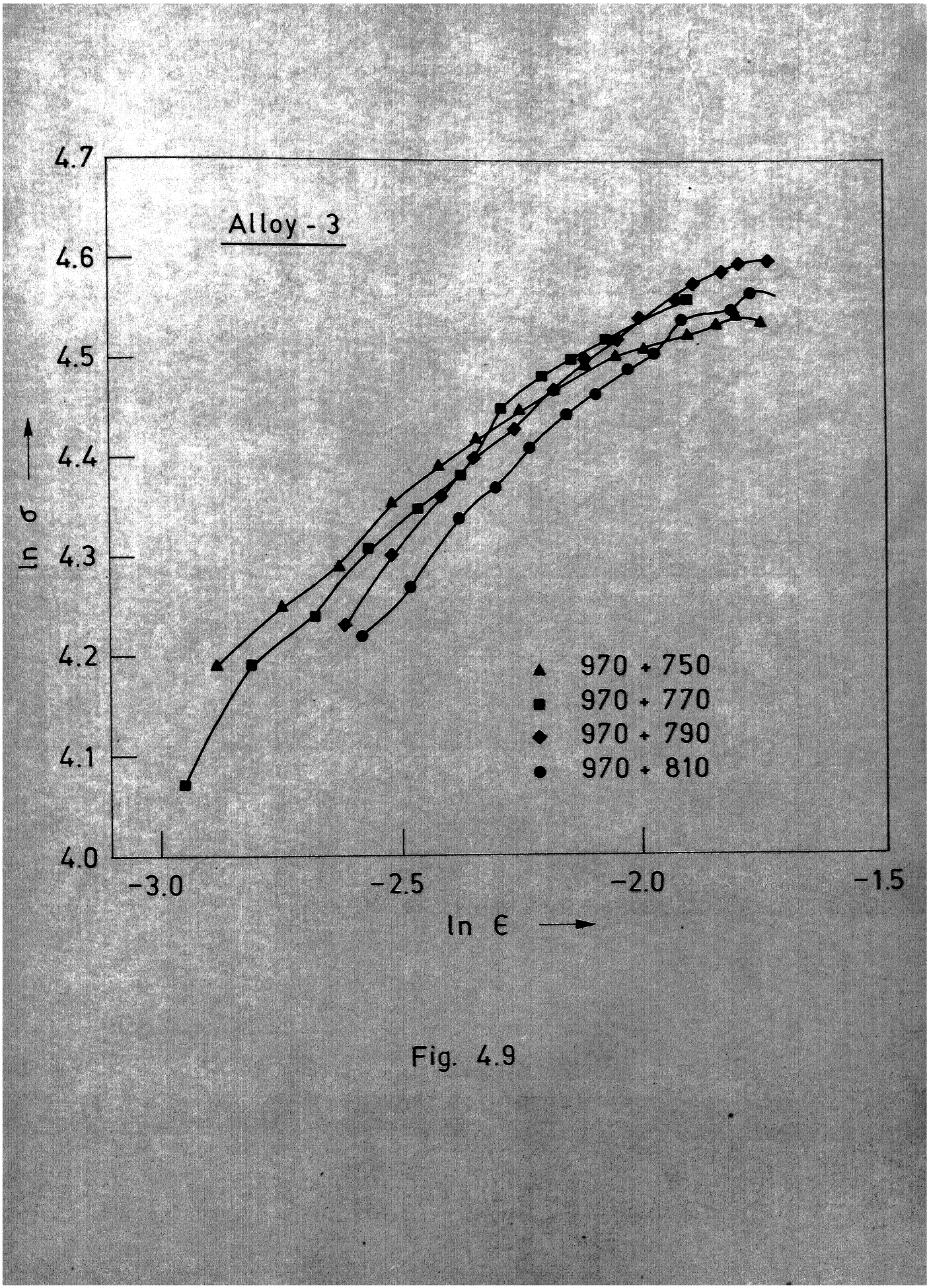
Alloy - 3
4.7
4.6
4.5
4.4
4.3
4.2
4.1
4.0
ln σ
-3.0
-2.5
-2.0
-1.5
ln ϵ
970 + 750
970 + 770
970 + 790
970 + 810

Fig. 4.9

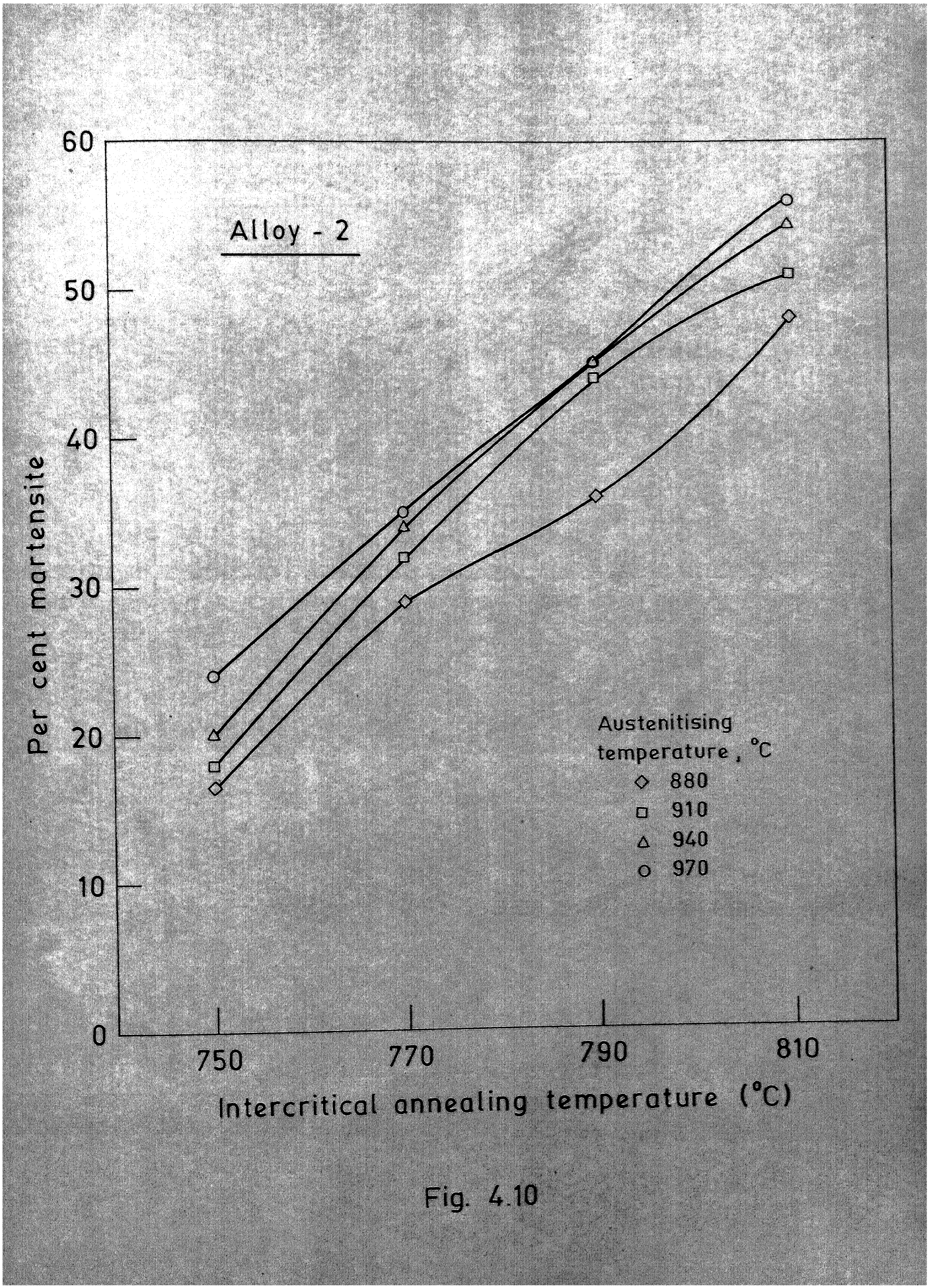
Alloy - 2
Per cent martensite
60
50
40
30
20
10
0
750
770
790
810
Intercritical annealing temperature (°C)
Austenitising temperature, °C
880
910
940
970

Fig. 4.10

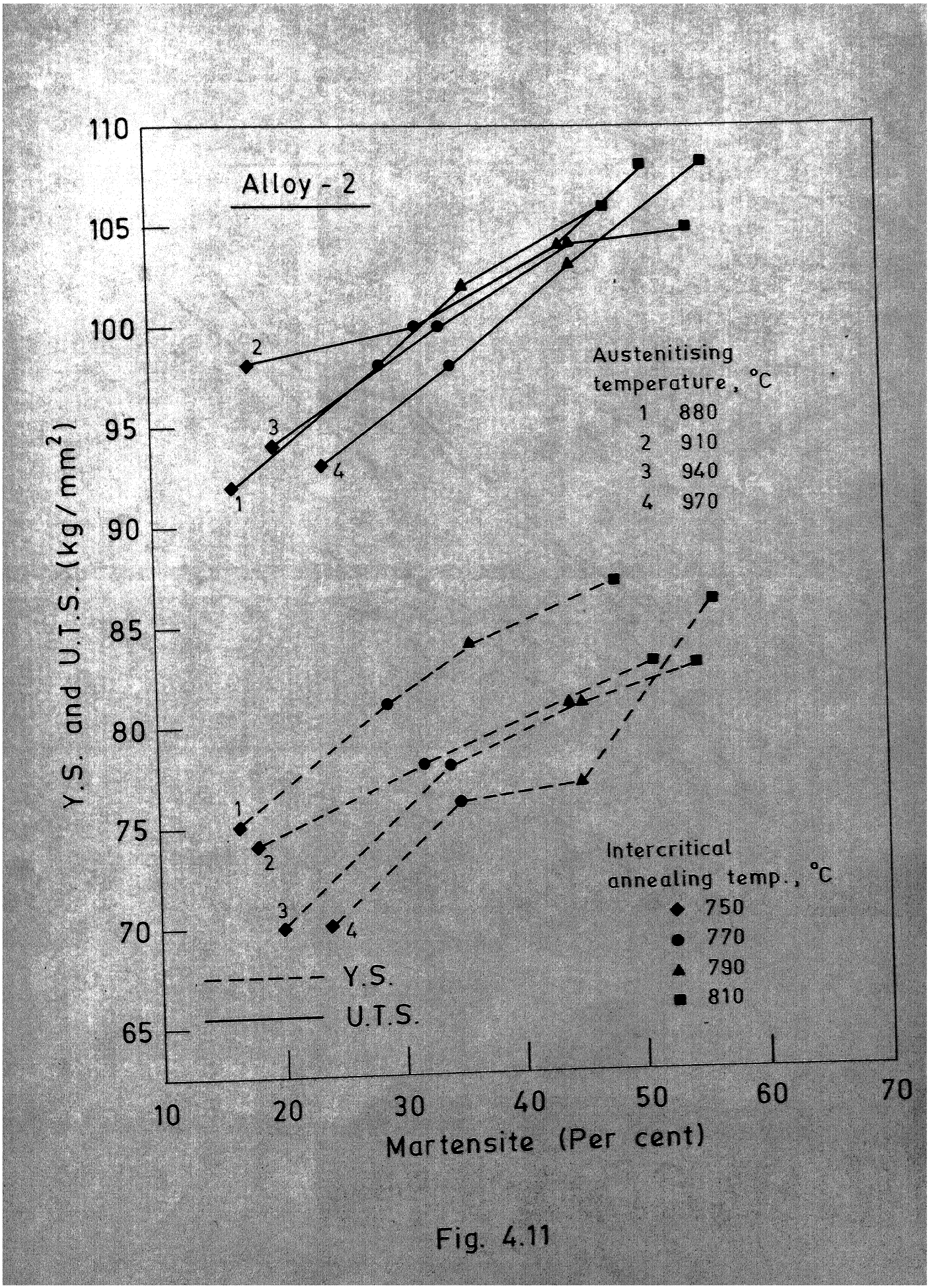
Alloy - 2
Austenitising temperature, °C
1 880
2 910
3 940
4 970
Intercritical annealing temp., °C
750
770
790
810
Y.S.
U.T.S.
Y.S. and U.T.S. (kg/mm²)
Martensite (Per cent)
110
105
100
95
90
85
80
75
70
65
10
20
30
40
50
60
70

Fig. 4.11

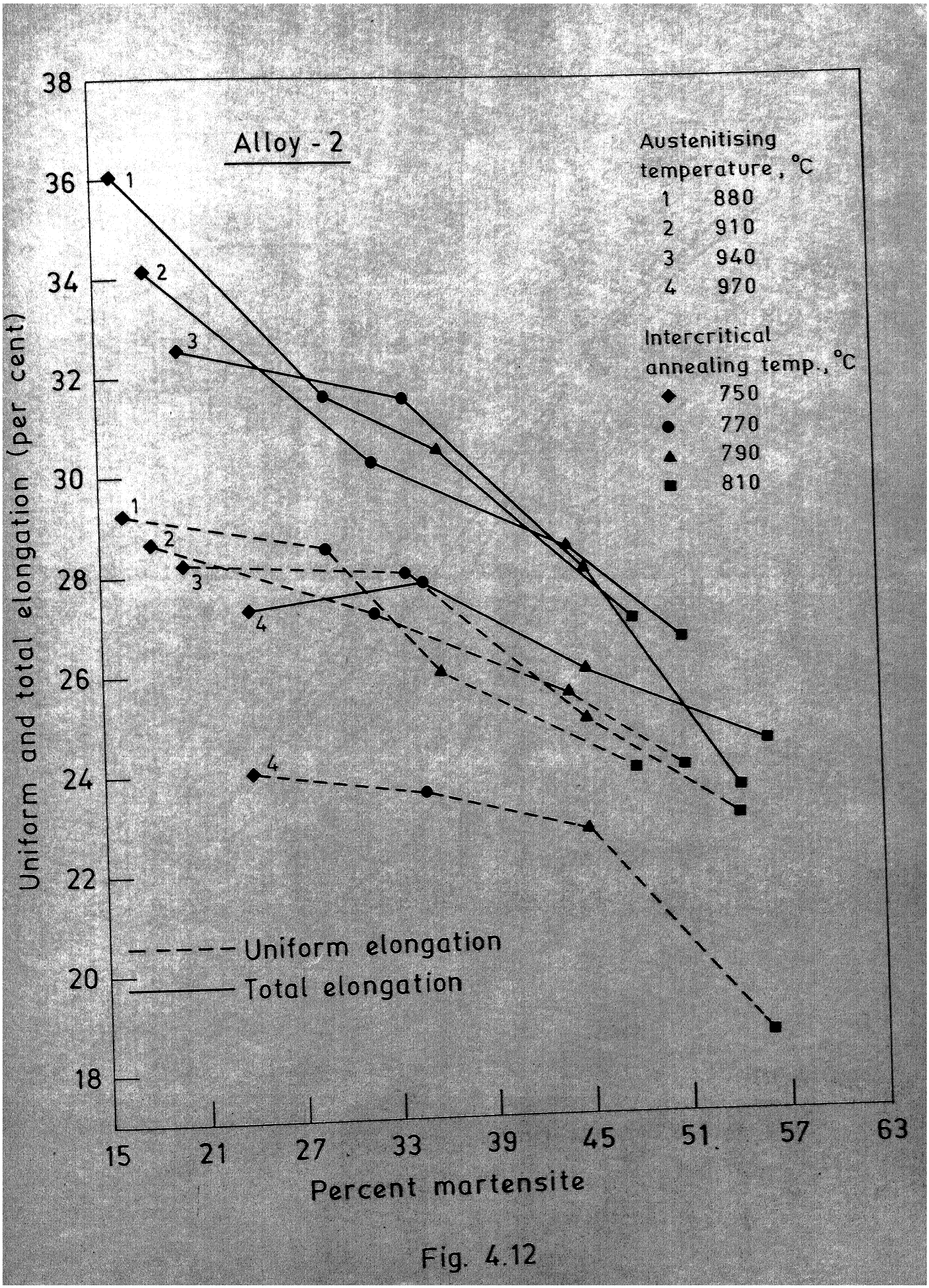
Alloy - 2
Austenitising temperature, °C
1 880
2 910
3 940
4 970
Intercritical annealing temp., °C
750
770
790
810
Uniform elongation
Total elongation
Uniform and total elongation (per cent)
Percent martensite
38
36
34
32
30
28
26
24
22
20
18
15
21
27
33
39
45
51
57
63

Fig. 4.12

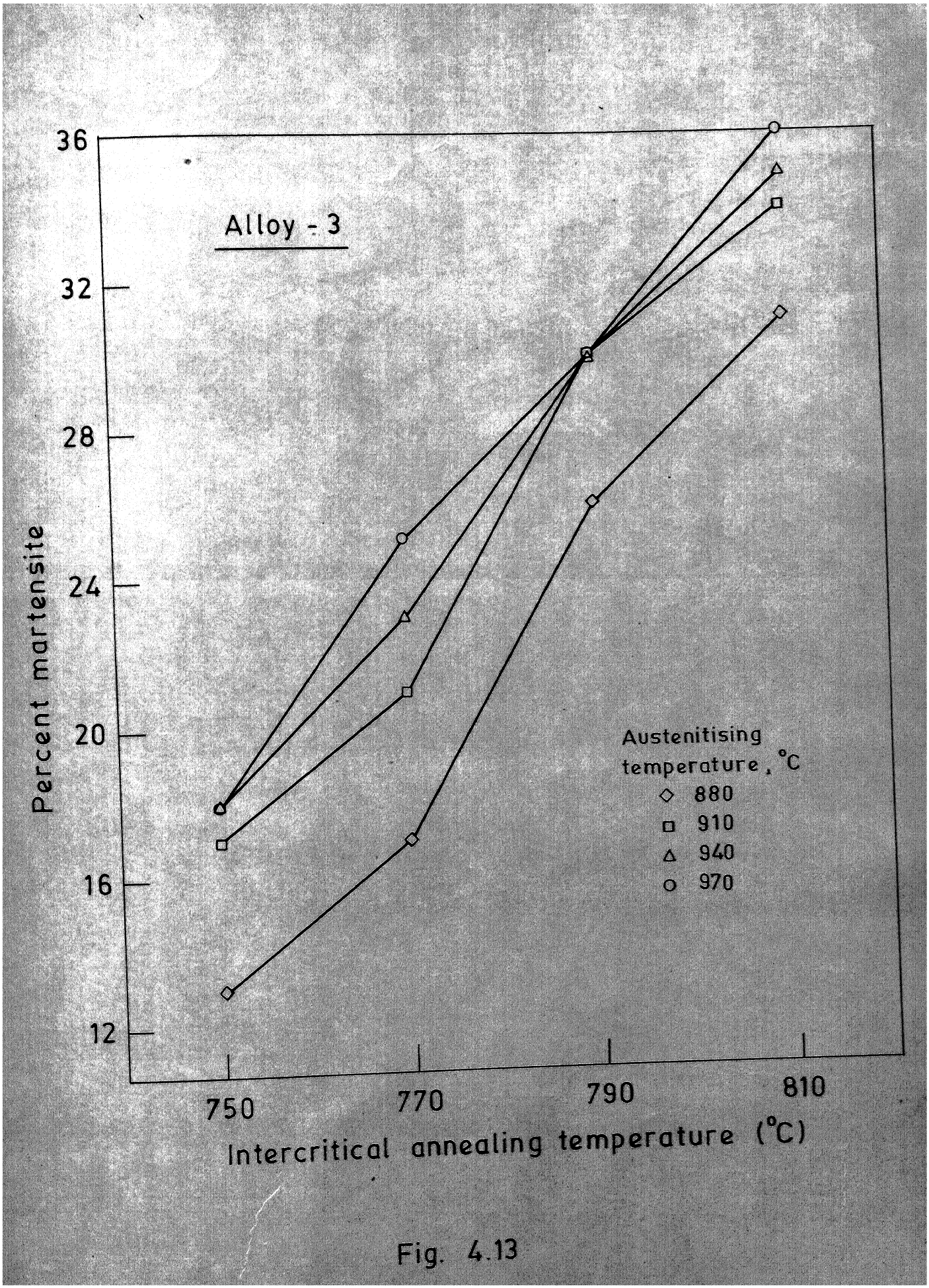
Alloy - 3
Percent martensite
36
32
28
24
20
16
12
750
770
790
810
Intercritical annealing temperature (°C)
Austenitising temperature, °C
880
910
940
970

Fig. 4.13

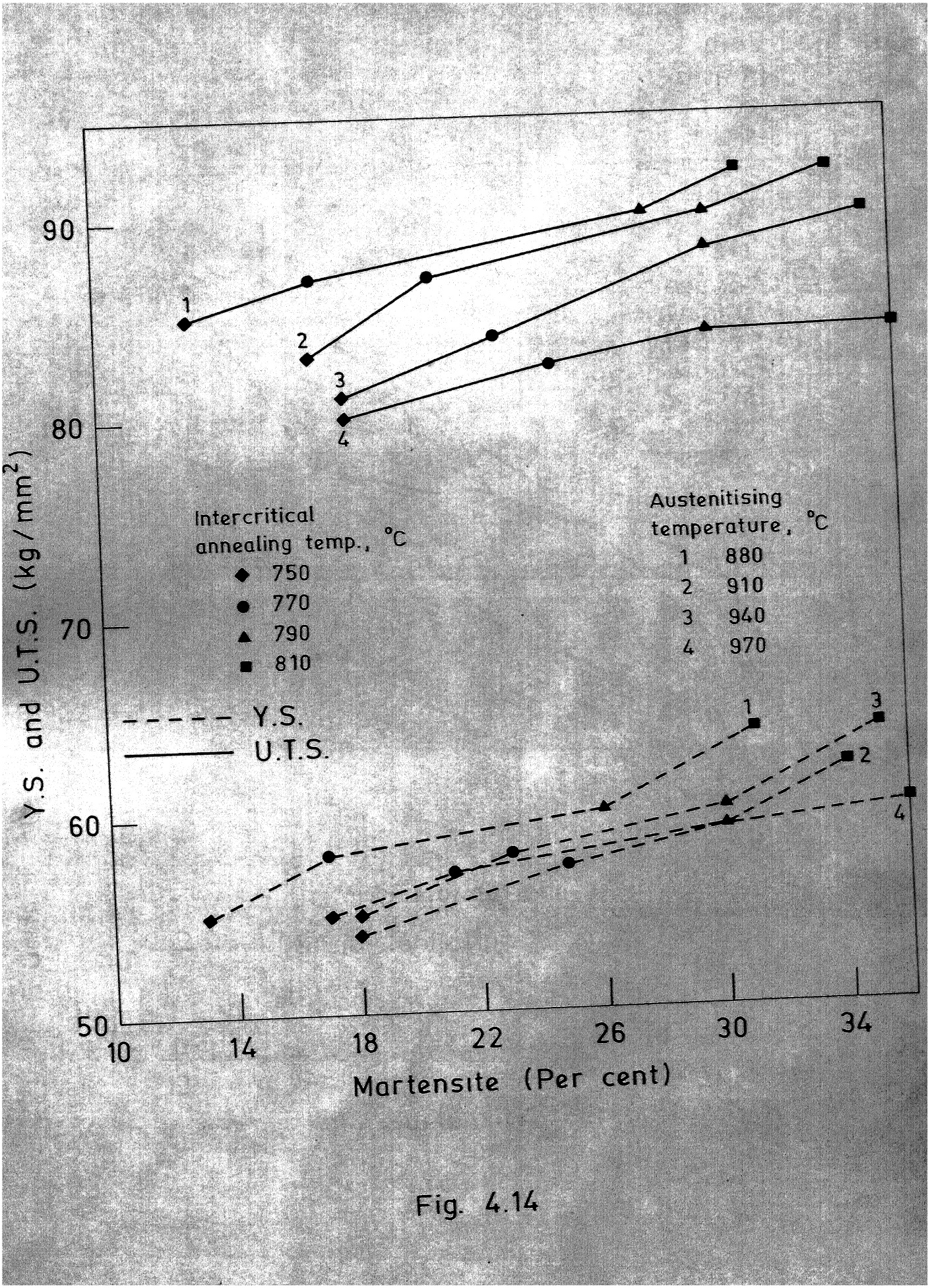
Y.S. and U.T.S. (kg/mm²)
90
80
70
60
50
10
14
18
22
26
30
34
Martensite (Per cent)
Intercritical annealing temp., °C
750
770
790
810
Austenitising temperature, °C
1 880
2 910
3 940
4 970
Y.S.
U.T.S.
1
2
3
4

Fig. 4.14

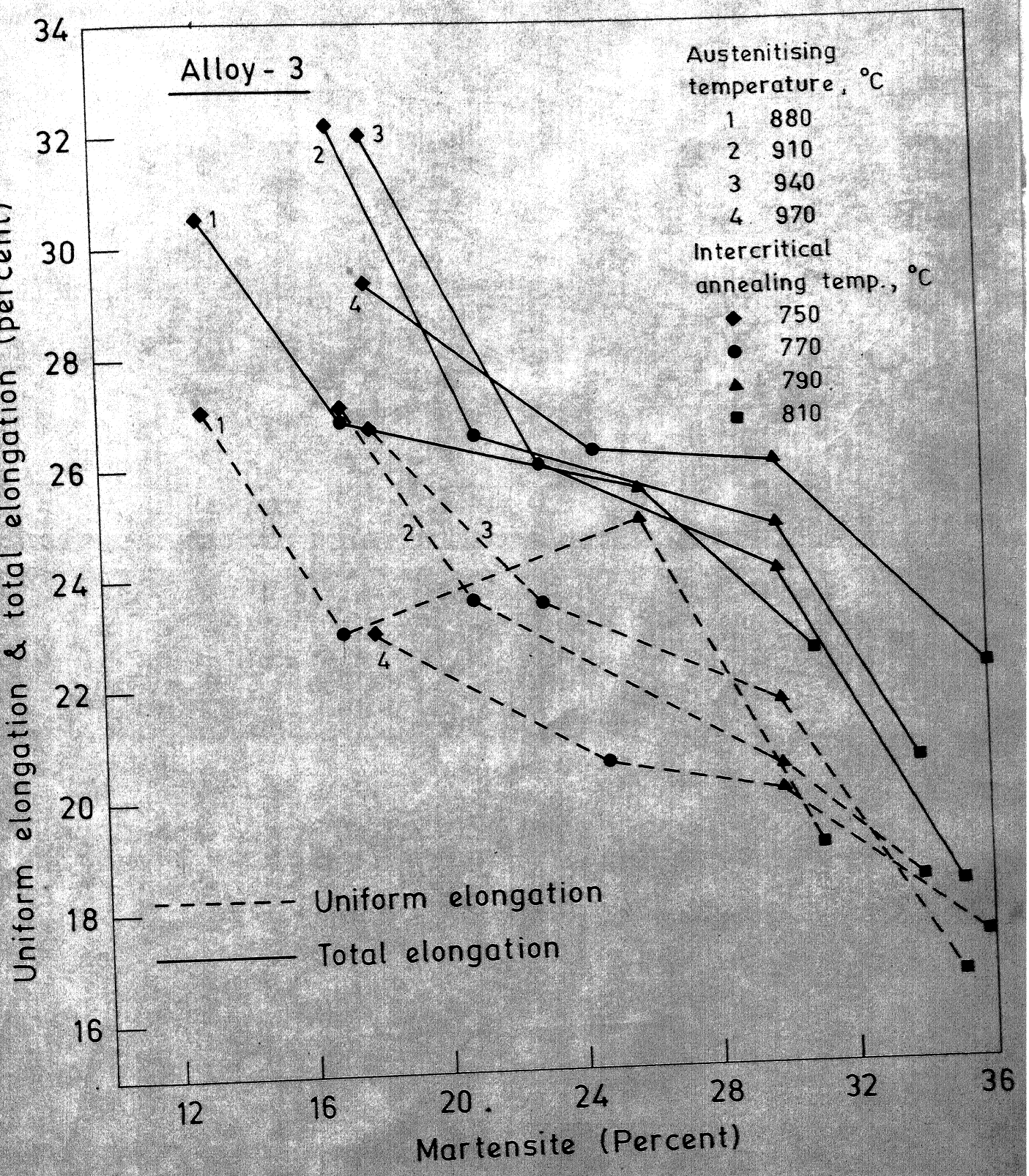
Alloy - 3
Austenitising temperature, °C
1 880
2 910
3 940
4 970
Intercritical annealing temp., °C
750
770
790
810
Uniform elongation
Total elongation
Uniform elongation & total elongation (percent)
Martensite (Percent)
34
32
30
28
26
24
22
20
18
16
12
16
20
24
28
32
36

Fig. 4.15

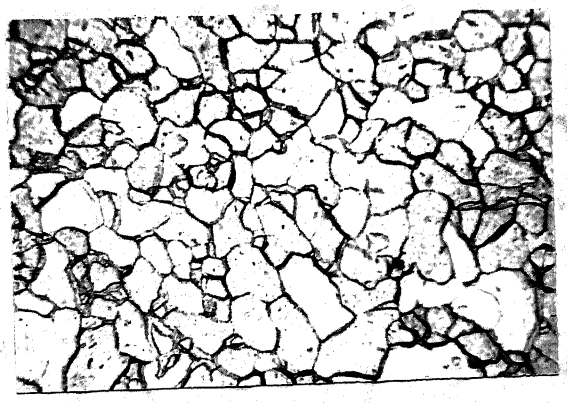

(a)

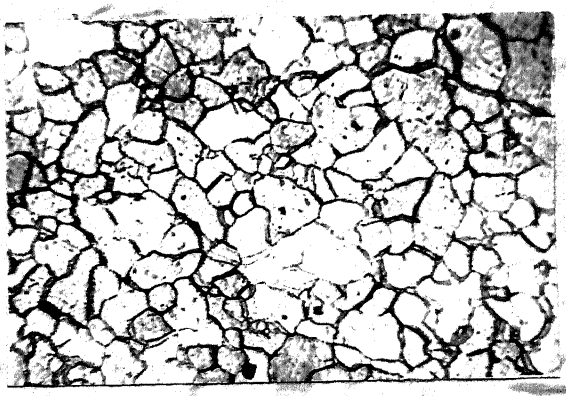

(b)

(c)

Fig.4.16

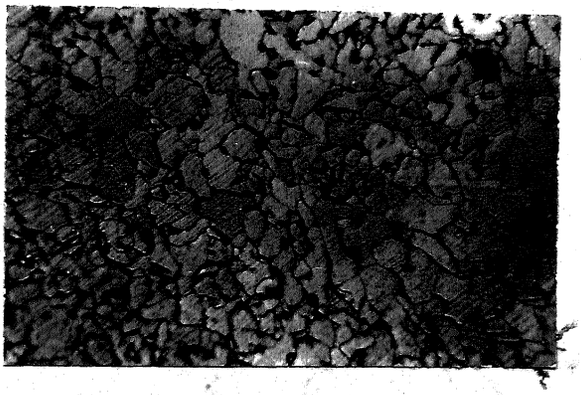

(a)

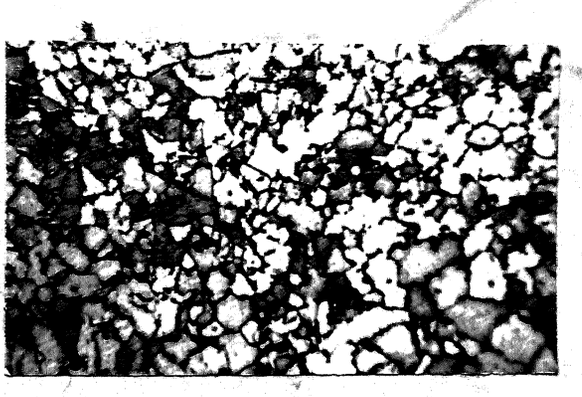

(b)

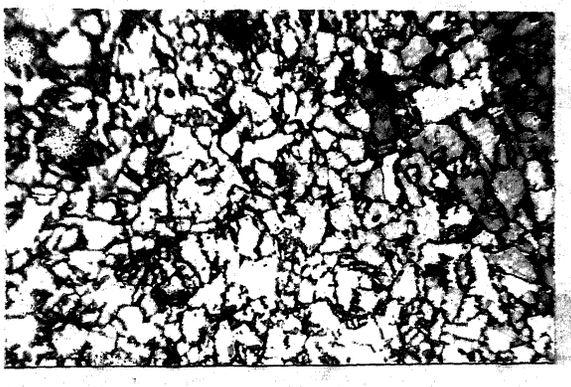

(c)

(d)

Fig.4.17

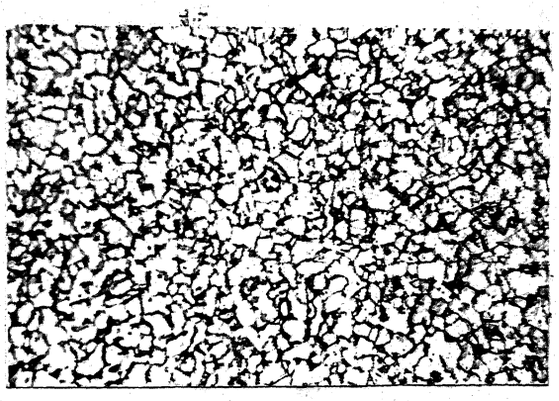

(a)

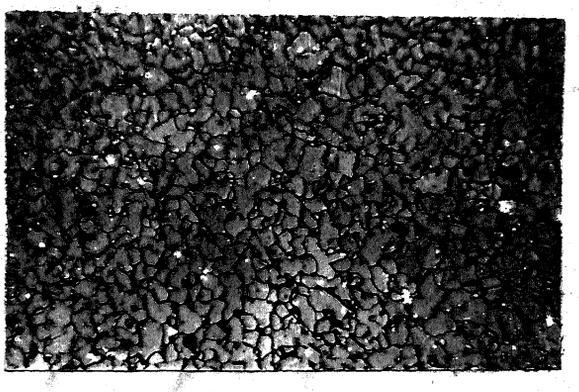

(b)

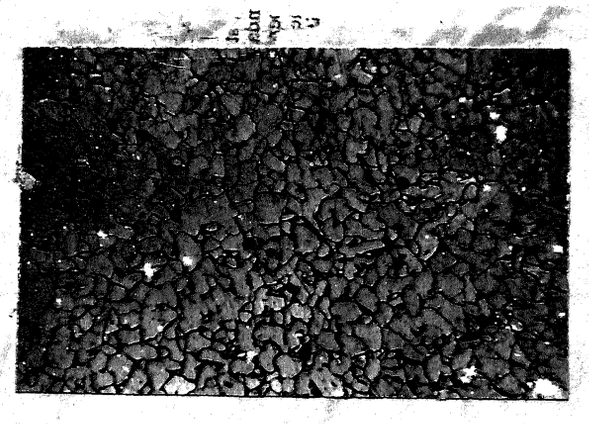

(c)

Fig.4.18

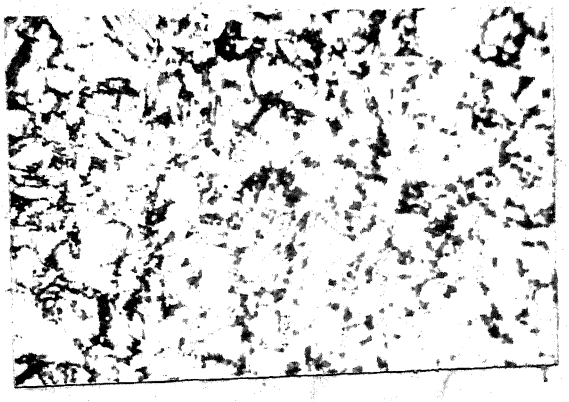

(a)

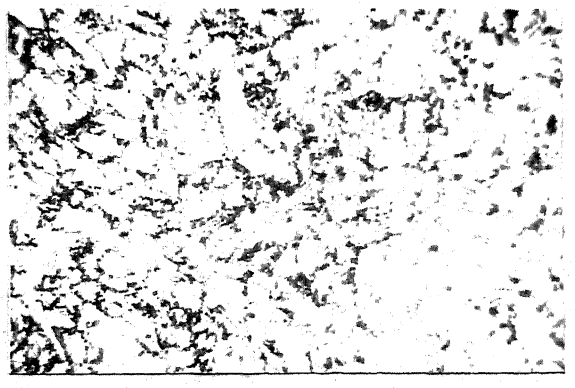

(b)

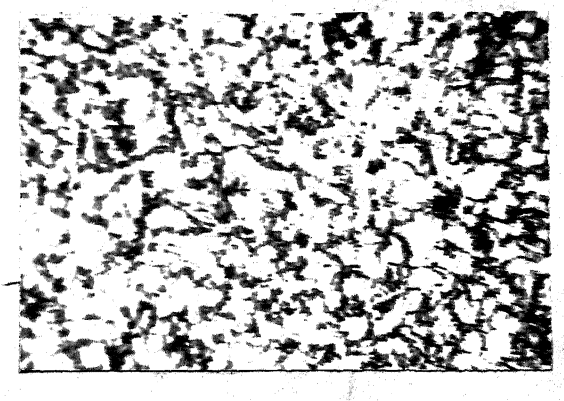

(c)

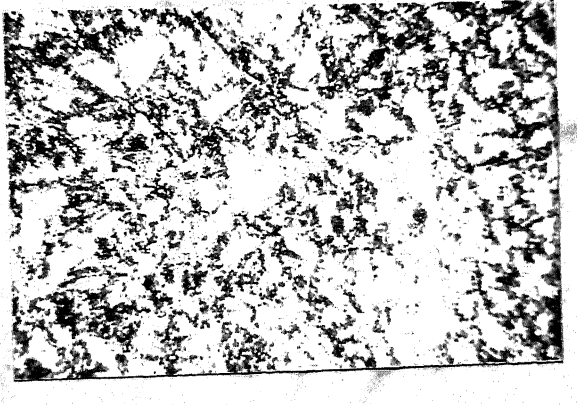

(d)

Fig.4.19

(a)

(b)

(c)

Fig.4.20

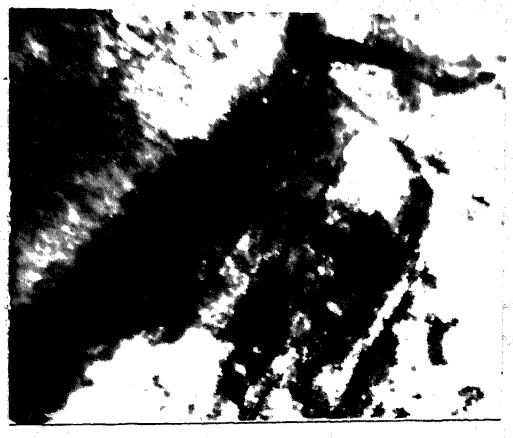

(a)

(b)

(c)

Fig.4.21

(a)

(b)

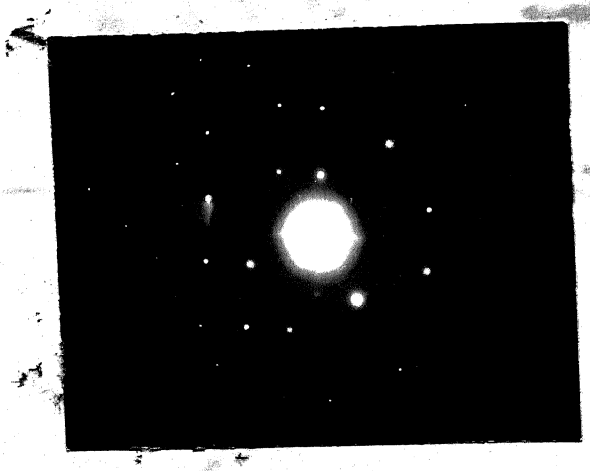

(c)

Fig.4.22

(a)

(b)

Fig.4.23

CHAPTER 5

DISCUSSION

In the present investigation it has been observed that after the two-stage heat-treatment alloy 1 assumes almost a single-phase structure consisting of ferrite only whereas alloys 2 and 3 show a dual-phase structure consisting of both ferrite and martensite.

That a dual-phase structure produces a much higher mechanical strength as compared to the single-phase ferritic alloy is borne out by the much higher Y.S. and U.T.S. values achieved in case of alloys 2 and 3 in comparison to alloy 1. The Y.S. and U.T.S. values between themselves are not found to change much for different heat treatments for the alloy 1. The strength in this alloy is presumably derived mostly from grain-size and solid solution strengthening of ferrite by silicon.

For a particular dual-phase heat-treatment the Y.S. and U.T.S. of alloy 2 are almost always found to have higher values, compared to alloy 3 (Figures 4.4 and 4.7). This has possibly happened due to two factors. Alloy 2 has almost double the amount of solute content compared to alloy 3. The extra solute is in the form of approximately 1.5% Si which is a good solid-solution hardener for ferrite.

Moreover, at any stage of heat-treatment the alloy 2 has a higher martensite content compared to alloy 3 (Figures 4.10 and 4.13). The higher amount of martensite in alloy 2 may be the reason for its higher strength values. That this is really so can be found out from Figures 4.11 and 4.14 which show the plots of Y.S. and U.T.S. against percent martensite for the alloys 2 and 3 respectively. The nature of the plots in these figures is very similar to the plots showing the variation of Y.S. and U.T.S. with the inter-critical annealing temperatures for these alloys (Figures 4.4 and 4.7). So higher strength within the same alloy system or between different alloy systems is found to be associated, invariably, with a higher volume fraction of martensite in the structure.

It may be seen in Figures 4.4 and 4.7 that the initial austenitising temperature also has some effect on the mechanical property values. Lower the austenitising the temperature higher are the values of Y.S. and U.T.S. normally. This is presumably due to a finer grain-size.

The uniform and total elongation(%) values for alloy 1 are found to be not much sensitive towards the inter-critical annealing temperature (Figure 4.2). However, a careful look suggests that these values are possibly slightly impaired with increasing inter-critical annealing temperature. As mentioned previously, in this alloy also

a little amount of the hard and brittle martensite phase is present at a few places mainly in the grain boundary regions of the ferrite grains although by optical microscopy it was found impossible to detect it. The gradual decrease of elongation (%) values with increasing inter-critical annealing temperature may have something to do with increasing martensite content in the specimens - however, small their total volume fraction may be.

In general, the uniform and total elongation (%) values for alloy 3 have been found to be very similar to those of the alloy 1 whereas the corresponding values for alloy 2 are slightly better (Figures 4.2, 4.5, 4.8). Elongation values are found to decrease with increasing inter-critical annealing temperature and with volume fraction martensite present. This is quite natural to expect.

In the course of the present investigation it was observed that all the three alloys have a low initial flow stress and their stress-strain curves show a continuous yielding behaviour. The deformation behaviour of a dual-phase steel has been characterised by its 'strain-hardening exponent' or n-value by a large number of investigators. In fact, it has been assumed by many that dual phase steels obey the Hollomon[25] relationship.

$$\sigma = K\varepsilon^n$$

where σ is the true stress, ε the true strain and K and n

are constants. From the above relationship, it is clear that if ln σ is plotted against ln ε, the slope of the resulting curve should yield the value of n, the strain-hardening exponent. It was with this idea that a plot of ln σ versus ln ε was made for each of the alloys austenitised at 970°C and given the dual-phasing heat-treatment (Figures 4.3, 4.6 and 4.9). It is quite clear from these plots that the data are not linear indicating that a single value of 'n' does not adequately describe the deformation behaviour of dual-phase steels. Similar observations were also made by Ramos et.al.[1].

As mentioned before the stress-strain curves for the present dual-phase steels do not exhibit any discontinuous yielding - rather yielding is continuous and smooth. This may be attributed to the gettering action of the vanadium in removing interstitial solutes from the matrix. The other reason is the abundance of free dislocations produced at a relatively low temperature by the martensitic transformation.

The rapid work-hardening after initial yielding (high n-value) may be explained by, (a) dislocation-dislocation interaction and (b) dislocation-precipitate (or cluster) interaction. The precise mechanism operative in the present series of alloys cannot be stated with confidence because of lack of work in this direction.

Mileiko[10] and Garmong and Thompson[26] have developed a theory of the mechanical properties of fibre-composites of two ductile phases tested in tension parallel to the fibre-axis; good agreement between experiment and theory was found for Ni-W, Cu-W and Ag-stainless steel composites. It has been shown[2] that the changes in tensile strength and ductility of dual phase steels as a function of the percent martensite are in agreement with this theory even though the martensite is not in a fibrous form. The values of the tensile strength and ductility of the component ferrite and martensite used to compare experiment with theory were obtained by extrapolation.

In Mileiko's theory, there are two assumptions as to materials properties. These are:

(1) The bond between fibre and matrix is ideal, so that the strength of the interface is sufficient to prevent the fibre necking without necking of the composit as a whole, that is, the more stable matrix restrains the less stable fibre. The interface in dual-phase steel is atomic in nature and therefore meets this requirement.

(2) The relationship between stress and strain for both the composite and components is a power law of the form $\sigma = K \varepsilon^n$ where σ is the true stress, ε the true strain and K and n are constants. It has been demonstrated[2] that dual phase steels follows reasonably well such a power law.

Mileiko[10] and Garmong and Thompson[26] have developed a theory of the mechanical properties of fibre-composites of two ductile phases tested in tension parallel to the fibre-axis; good agreement between experiment and theory was found for Ni-W, Cu-W and Ag-stainless steel composites. It has been shown[2] that the changes in tensile strength and ductility of dual phase steels as a function of the percent martensite are in agreement with this theory even though the martensite is not in a fibrous form. The values of the tensile strength and ductility of the component ferrite and martensite used to compare experiment with theory were obtained by extrapolation.

In Mileiko's theory, there are two assumptions as to materials properties. These are:

(1) The bond between fibre and matrix is ideal, so that the strength of the interface is sufficient to prevent the fibre necking without necking of the composit as a whole, that is, the more stable matrix restrains the less stable fibre. The interface in dual-phase steel is atomic in nature and therefore meets this requirement.

(2) The relationship between stress and strain for both the composite and components is a power law of the form $\sigma = K \varepsilon^n$ where σ is the true stress, ε the true strain and K and n are constants. It has been demonstrated[2] that dual phase steels follows reasonably well such a power law.

Thus, it has been suggested that dual-phase steels fulfil the materials criteria for the applicability of the theory to experimental data, although they do not fulfil the geometric requirement of fibres aligned parallel to the tensile axis.

On the basis of the present work as well as work by Ramos et.al.[1] it is doubtful whether a single-value of n can be used for the entire stage of deformation of dual-phase steels.

According to Mileiko's theory, the tensile strength of the composite σ_c will be given by the following expression:

$$\sigma_c = V \lambda' \sigma_m + (1-V) \lambda'' \sigma_f$$

where $\lambda' = (\varepsilon_c/\varepsilon_m)^{\varepsilon_m} \exp(\varepsilon_m - \varepsilon_c)$

and $\lambda'' = (\varepsilon_c/\varepsilon_f)^{\varepsilon_f} \exp(\varepsilon_f - \varepsilon_c)$

In these expressions, σ_m and σ_f are the tensile strengths of the martensite and ferrite respectively; and ε_c and ε_f and ε_m are the true uniform strains for the composite, ferrite and martensite respectively. V is the volume fraction of martensite present in the material.

Some simple calculations were performed to find out if this theory also holds good for the present alloys.

Let us, for example, take the case of the alloy 2 which has been initially austenitised at 970°C and then intercritically annealed at 770°C. V in this case (Figure 4.10) is 0.35 and ε_c has been calculated to be 0.1862. The following theoretical values for σ_m, σ_f, ε_m and ε_f have been used in this work[6].

σ_m = 204 Kg/mm^2, σ_f = 42 Kg/mm^2, ε_m= 0.07 and ε_f = 0.31.

Based on these values λ' comes to be 0.95 and λ'' has a value of 0.967. σ_c can then be calculated to have a value of 94.23 Kg/mm^2. From **Table** 4.2 the U.T.S. of **alloy** 2 at this stage of heat-treatment has been found out to be (by experiment) 98 Kg/mm^2. The agreement between the theoretical and the practical values is quite good.

Presumably in the above calculations the values of σ_m and σ_f that have been used refer to a very strong martensite and a very soft ferrite. It may be found out that if the values of σ_m and σ_f are taken from the results obtained from the present series of alloys, a simple law of mixture can satisfactorily explain the strength behaviour of the dual-phase steels. For example, the ferrite in the present case cannot be very soft, since it contains a good amount of solid solution hardener. Since alloy 1 in the present series is almost fully ferritic, it was thought that the strength of ferrite in alloy 2 should be comparable to the strength of the alloy 1 under identical conditions of heat treatment. For alloy 1, austenitised at 970°C and

then inter-critically annealed at 770°C, the U.T.S. has been found out to be 78 Kg/mm^2 (Table 4.1). Again by extrapolation, from the relevant curve showing the variation of U.T.S. with volume fraction martensite in alloy 2 (Figure 4.11), the U.T.S. of the alloy with 100% martensite in it can be found out to be 122 Kg/mm^2. Now, according to the simple 'law of mixture', the tensile strength of the composite σ_c will be given by

$$\sigma_c = V \sigma'_m + (1-V)\sigma'_f$$

where V is the volume fraction of martensite in the microstructure, σ'_m is the tensile strength of the martensitic phase and σ'_f the tensile strength of the ferritic phase in the composite microstructure. Here V = 0.35, σ'_m = 122 Kg/mm^2, σ'_f = 78 Kg/mm^2.

$$\text{Hence, } \sigma_c = (0.35 \times 122 + 0.65 \times 78) \text{ Kg/mm}^2$$
$$= 93.40 \text{ Kg/mm}^2.$$

The experimental value of σ_c at this stage, as mentioned before is 98 Kg/mm^2. Thus the agreement between the theoretical and practical values are quite satisfactory.

Similar arguments were also obtained for the tensile strength values for alloys 2 and 3 after various heat treatment schedules.

CHAPTER 6

CONCLUSIONS

(1) Dual-phase microstructure could be developed in a 0.1% C - 1.5% Mn steel (alloy 3) as well as a 0.1% C - 1.5% Mn - 1.5% Si steel (alloy 2) whereas the steel with 0.1% C - 1.5% Si (alloy 1) was almost fully ferritic.

(2) The mechanical properties developed in the steels with dual-phase structures were found to be much superior to that of the alloy containing ferrite only.

(3) The stress-strain curves of the dual-phase steels show a continuous yielding behaviour and rapid strain-hardening characteristics.

(4) The strengths developed in alloys 2 and 3 are very much a function of the martensite content in the microstructure- the higher the martensite volume fraction more is the strength.

(5) The strain-hardening exponent 'n' has not been found to have a constant value throughout the deformation process. Variation of the 'n' value suggest that the deformation must be taking place in several well-defined stages.

(6) The calculated strengths of the dual-phase steels on the basis of theoretical models have been found to tally well with the corresponding experimental values.

LIST OF REFERENCES

1. Luis F. Ramos, David K. Matlock and George Krauss, "Communication of the deformation behaviour of dual phase steel", Metallurgical Transaction, Vol.10A, February 1979.

2. R.G. Davies, "Influence of martensite composition and content on the properties of dual phase steels", Metallurgical Transactions, Vol.9A, May 1978.

3. R.G. Davies, "The deformation behaviour of vanadium strengthed dual phase steel", Metallurgical Transactions, vol.9A, January 1978.

4. R.G.Davies, "The mechanical properties of zero-carbon ferrite plus martensite structures", Metallurgical Transactions, vol.9A, March 1978.

5. Prof. R. Lagneborg, "Seminar on vanadium cold processing and dual phase steels", Paper presented on the invitation of Gessellschaft fur Elektrometallurgie, West Berlin, October 1978.

6. R.G. Davis and C.L. Magee, "Seminar on vanadium cold processing and dual phase steels", Paper presented on the invitation of Gessellschaft fur Electrometallurgie, West Berlin, October 1978.

7. J.H. Bucher and E.G. Hamburg, "SAE 770164", Int.Automotive Engineering Congress, Detroit, Feb.-March, 1977.

8. P.R. Mould and C.C. Skeena, "Structure and properties of cold rolled ferrite martensite steel sheets", presented at Symposium - Modern development in HSLA formable Steels", AIME Chicago, Oct. 1977.

9. J.D. Boyd, "Materials engineering in the Arctic", Ed. M.B.Ives, ASM Metal park, Ohio, 44073, p.200, 1977.

10. S.T.Mileiko, "The tensile strength and ductility of continuous fibre composites", J. Mat.Sc., Vol.4(1969), pp. 974-977.

11. P. Ostrom and I. Lindgren, "Relationship between microstructures and mechanical properties of a vanadium and plain carbon dual phase steel, Swedish Institute for Metals Research, IM-1308, Aug.1978.

12. K. Araki, Y. Takada, K. Nakada, "Work hardening of continuously annealed dual phase steels", Trans. ISIJ, 17(1977), pp. 710-717.

13. R.G. Davies, "Conference on Modern developments in HSLA Formable steels", AIME Chicago, October 1977.

14. R.G. Davies, "Influence of Silicon and phosphorous on the mechanical properties of both ferrite and dual phase steels", Met.Transaction, Vol.10, Jan. 1979.

15. A.M. Sherman and R.G. Davies, Met. Trans. to be published.

16. J.M. Rigsbee Vander, P.J. Arend, "Laboratories studies of microstructure and structure property relations in dual phase HSLA steels", Republic Steel Corpn. Research Centre, PR-12, 050-78.3, May 1978.

17. R.F. Hehemann, "Phase transformations", American Society for Metals, 1968, p. 397.

18. M.S. Rashid, "GM980X - A unique high strength sheet steel with superior formability", General Motor Comp., Research Lab., GMR-1044, Feb. 1976.

19. J.M. Morrow, G. Tither, R.M. Buck, "Intercritically annealed dual phase steels for automotive applications", Climax Molybdenum Comp Research Lab., L-176, 182, March 1978.

20. P.E. Repas, "Seminar on vanadium cold processing and dual phase steels", Paper no.2, On the invitation of Gessellschaft fur Electrometallurgie, West Berlin, Oct. 1978.

21. R.G. Davies, "On the ductility of dual phase steels", Ford Motor Company, Deaarborn, Michigan.

22. K. Makaoka, K. Araki and K. Kurihara, "Strength, ductility and ageing properties of continuously annealed dual-phase high strength sheet steels", Nippon Kokkan K.K. Paper Presented at the AIME, Fall Meeting, Oct. 1977.

23. B. Carlsson, and B. Sundstrom, "Inhomogeneity in plastic deformation of two phase steels", Materials Sc. and Engg., 16(1974), pp. 161-168.

24. H. Masui, H. Takeschi, "On the combination of tensile strength and ductility in the high strength cold rolled steels and the metallurgical factors responsible therefore", Trans. ISIJ 16(1976), pp. 161-168.

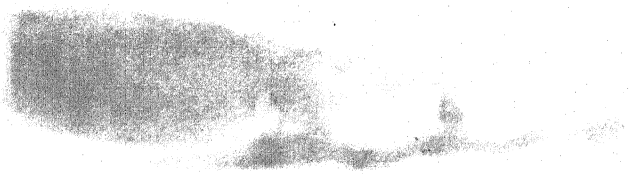

25. J.H. Hollomon, Trans. AIME, 1945, Vol.162, p.268.

26. G. Garmong and R.B. Thompson, Met. Trans. 1973, Vol. 4, p. 863.

27. W.B. Morrison, Trans. ASM, 1966, Vol. 59, p. 824.